UNIVERSITY OF ZULULAND

Synthesis of Cobalt (II) Schiff Base Complexes: Potential Precursors for Cobalt and Cobalt Sulfide Nanoparticles

A dissertation submitted by

Sandile Humphry Khoza

(206000208)

to the Faculty of Science and Agriculture in fulfilment of the requirements for the award of the degree of

Master of Science

in the Department of Chemistry

University of Zululand

(March 2017)

Supervisor: Prof. N. Revaprasadu

DECLARATION STATEMENT

I hereby declare that the work on the "Synthesis of cobalt (II) Schiff base complexes: Potential precursors for cobalt and cobalt sulfide nanoparticles" is my own work, which was conducted in the Department of Chemistry at the University of Zululand. I declare that all the sources I have quoted have been indicated and acknowledged by means of complete references.

……..

Sandile Humphry Khoza

ACKNOWLEDGEMENTS

First I would like to thank God, the Almighty for all His blessings. To Prof. Neerish Revaprasadu, thank you so much for your guidance and supervision of my work. Thank you for your inspiration and care through frustrating times and thank you for all your time you committed to all my needs.

To the Late Dr. Nejo, thank you very much for the project and the continuation of your work as a research student, I will always cherish the moment you spent with me and I hope this work we did together will have a great impact in future. To Dr. Seqapelo, thank you so much for all your support and advice you gave me when I had a problem, thank you very much. I would like to thank Dr. Mlowe for his assistance and his support. Thank you for your invaluable advice and guidance throughout the years.

I would like to thank all my colleagues (nano group) for their support, especially to Siphamandla Masikhane for his assistance in my research and as a friend. Thanks for being there when I had personal problems.

My sincere words of gratitude go to my dad, Mr. M. S. Khoza, thank you for your support, understanding and allowing me to reach for the stars. To my mom (Miss R. Rose dos Santo Virchane) and my step mom (Miss L. Sibambo), thank you for getting me started a few years back, if it wasn't for you I wouldn't be here today. Your support and motherly advice has kept me going for all these years. To my siblings Adolph, Petro, Titus, Thobile, Sis-Thobile, Veronica and Ayanda thank you for your support and love.

My truthful words of thankfulness to the NRF for financial support.

This dissertation is dedicated

to

my parents and my sons

(Lwandiswa and Lugqabho)

ABSTRACT

Schiff bases ligands and their cobalt complexes have been widely studied due to their attractive chemical and physical properties, which enables exploitation in a multiplicity of applications in several scientific areas. Metal and metal sulfide nanoparticles are useful in many applications as they exhibit different particle sizes, shapes and surface-to-volume ratios. Several methods for the preparation of metal and metal sulfide nanoparticles have been established. In this project, cobalt and cobalt sulfide nanoparticles were selected and synthesized because of their unique properties and applications. The use of single source precursors for the synthesis of nanoparticles have been used by methods such as hot injection and pyrolysis.

The synthesis of three Schiff base ligands namely; N,N'-bis(1-naphthaldehyde)-4-methylorthophenylenediimine [Ligand (**1**)], N,N'-bis(5-methoxybenzaldehyde)-4-methylorthophenylenediimine [Ligand (**2**)] and N-(naphthaldehyde)- N'-(3-methylbenzylidene)benzoic acid [Ligand (**3**)], leads to the formation of three Schiff base cobalt(II) complexes namely; N,N'-bis(1-naphthaldehyde)-4-methylorthophenylenediiminatocobalt(II) [Complex (**4**)]; N,N'-bis(5-methoxybenzaldehyde)-4-methylorthophenylenediiminatocobalt(II) [Complex (**5**)] and N-(naphthaldehyde)- N'-(3-methylbenzylidene)benzoic cobalt(II) [Complex (**6**)]. The complexes (**4** and **5**) were used as single source precursors (SSPs) for the fabrication of cobalt nanoparticles by the hot injection and the pyrolysis routes. For the fabrication of cobalt sulfide, only the hot injection route was used. The variation of parameters such as reaction time and temperature were used to determine their properties.

The morphology, composition, structural and magnetic properties of the as-synthesized nanoparticles were found to depend on the reaction conditions used during the synthesis. The

morphology and structural properties of the cobalt and cobalt sulfide nanoparticles were investigated using different techniques. Nanorods and cubic-like shaped Co nanoparticles which are indexed to a mixture of cobalt and cobalt oxide phases, were observed. Furthermore, the as-synthesized Co nanoparticles showed ferromagnetic behaviour. The use of 1-dodecanethiol as sulfur source afforded the formation of cobalt sulfide nanoparticles when complex (**6**) was used as single source precursor. The X-ray diffraction, high resolution transmission electron microscopy and selected area electron diffraction confirmed the formation of cubic Co_9S_8 and Co_3S_4 phase.

Table of Contents

List of Figures

List of Tables

ABBREVIATIONS

NPs	nanoparticles
MNPs	metal nanoparticles
SSPs	single source precursors
ICDD	international center for diffraction data

Chemical reagents

HDA	hexadecylamine
TEA	triethylamine
TOP	tri-n-octylphosphine
DDT	1-dodecanethiol

Instrumentation

FT-IR	fourier transform infrared spectroscopy
HRTEM	high resolution transmission electron microscopy
TEM	transmission electron microscopy
SEM	scanning electron microscopy
XRD	X-ray diffraction

TGA	thermogravimetric analysis
NMR	nuclear magnetic resonance
EDX	energy dispersive X-ray analysis
SAED	selected area electron diffraction

Chapter 1

Literature Review of Metal Schiff Bases and Metal Nanoparticles

Chapter 1

PART I 1.1. INTRODUCTION

Contents

1.1. Background review

1.1.1. Nanotechnology

Nanotechnology is a multidisciplinary field which is largely dominated by scientific disciplines such as chemistry, physics, engineering, computer science, biology and medicine [1]. Nanotechnology by definition is a term for designing, characterization, fabrication and application of structures, devices and systems by controlling shape and size at the nanometer scale [2]. Particles smaller than 100 nm in diameter are frequently considered as nanoparticles. Figure 1.1 shows how nanoparticles compare to other biological entities at the micro scale. The nano-sized particles exhibit unique electronic, magnetic, optical, and chemical properties due to quantum-size effects [3-6].

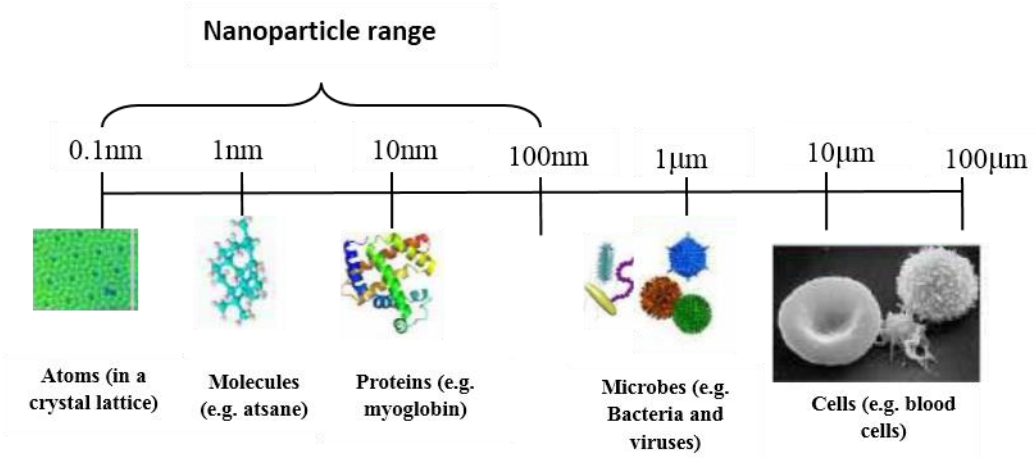

Figure 1.1: Nanoparticles in comparison with other biological entities [4].

1.1.2. Properties of nanoparticles

The observed properties of nanoparticles are as a result of their physical state (size, shape and morphology) which influence their electronic behaviour. A decrease in particle size approaching the nanometer size region, also promotes an increase in the surface area to volume ratio of particles in a material [7]. In general many articles show that by adjusting the reaction parameters (such as temperature, time and concentration of the reagent and the concentration of the stabilizing surfactant) systematically lead to control of particle sizes [8]. In general particle sizes increase with increasing time (more monomeric species are produced) and temperature (due to increased rate of reaction) [9]. The important issue for the shape control of nanoparticles is to generate anisotropic nanoparticles. For example, anisotropic magnetic nanoparticles are expected to offer many advantages since shape anisotropy has an influence on the magnetic properties. The approach to produce shape anisotropy during nanoparticle growth is by stabilizing a specific facet through molecular interactions. The control of nanoparticle shapes provides a well-designed strategy for optical tuning [10].

The shape of the particle also influences physical and electronic properties of inorganic nanomaterials. The observed shape of a nanoparticle is as a result of how unit cells arrange themselves in a specific lattice order. The lattice order arrangements are best grouped by their dimensionality parameters, which are basically faces along a Cartesian plane. There are four known dimensions (Figure 1.2), namely: zero-dimension (0D) refers to polyhedrons and spheres, one-dimension (1D) refer to wires and rod-like geometries (nanowire/nanorods,

nanoshuttles, nanocapsules and hollow structures), two-dimension (2D) refers to prism geometries and sheet-like nanocrystals (round disks, hexagonal/triangular quadrangular plates or sheets, belts, mesoporous-hollow nanospheres, hollow rings), and three-dimension (3D) refers to a continuous/network crystalline structure (nanourchins, nanoflowers, nanostars, polygonal nanoframes, multiple hollow shelled NPs, hollow bunches). Therefore, the dimensions assigned to specific geometries translate or associate to a number of planes that are not confined along the Cartesian plane, at which the nanocrystals grow in a self-assembly mechanism [7].

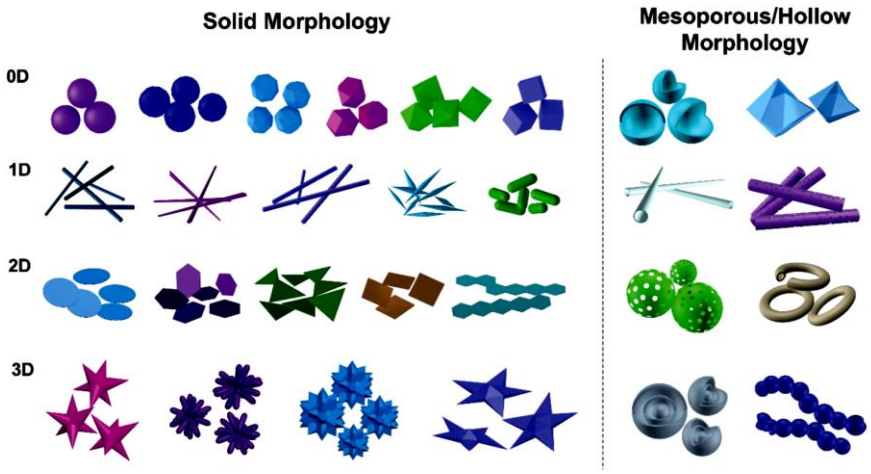

Figure 1.2: Typical morphologies of solid and hallow nanoparticles.

1.1.3. Metal nanoparticles (MNPs)

Nanotechnology-based research fields have shown an exponential increase in MNPs, as compared to other types of nanomaterials (Figure 1.3), simply due to the numerous properties which are relatively easy to harness [11]. MNPs can exhibit different particle sizes and shapes, as well as surface-to-volume ratios, which subsequently determine their applications in appropriate fields. Advances in applications such as in optics, electronics, catalysis, and biological systems, have been reported [12, 13].

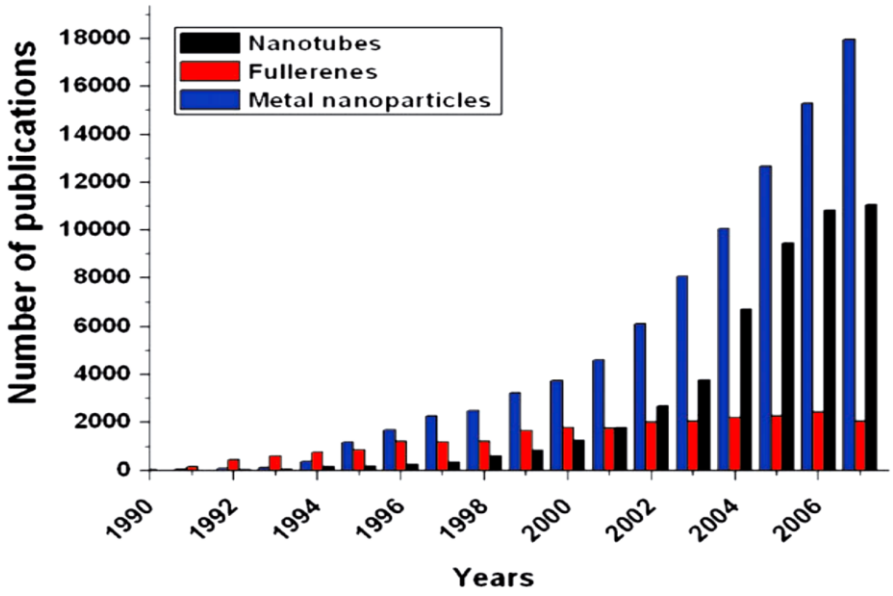

Figure 1.3: Growth in interest in Metal nanoparticles (as determined by number of citations) compared to nanotubes and fullerenes. (Source: ISI Web of Science) [14].

The plasmon resonances occur in MNPs, depending on the size and shape of the particles. Surface plasmon resonances (SPR) were reported as early as 1902 [15-17], where they were practically found in the application of sensitive detectors, which were capable to detect in sub-monomolecular coverage. It was observed that the phenomenon changed with the composition of the liquid when it interacts with the metal surface. In 1970, Rayleigh [18] proposed the *dynamical theory of grating*, which was based more on a clarification of the scattered electromagnetic field in relation to wavelength known as the Rayleigh wavelength, λ_R. Furthermore, Fano [19], Otto [20], Kretschmann and Raether [21] continued with the excitation studies of SPR. This consequently motivated an increase in interest and attention to applications of solid state physics, such as biosensing and solar cells.

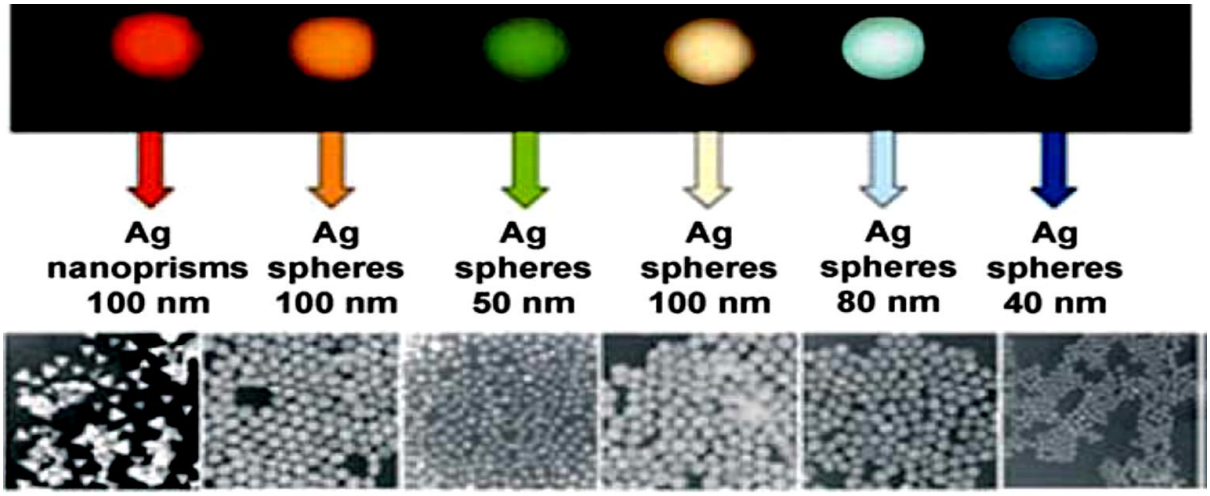

Figure 1.4: The influence of particle sizes on the optical properties of AgNPs [22].

The majority of MNPs emit light ot different wavelengths due to the collective oscillations of conduction band electrons, when excited by light of suitable frequencies (Figure 1.4). Since electrons are particles with an electric charge, they can easily vibrate, thus generating an additional electric field to that from the external source. When both electric fields resonate, the phenomenon is referred to as a surface plasmon resonance that takes place at the surface of the metal. In nano-optics, the optical properties of metal nanoparticles play a key role due to the localized surface plasmons with resonance wavelengths in the visible regime. Some metal nanoparticles are also known to have a great catalytic potential, owing to their ability to lower the activation energy of the reactants in certain reactions, thus facilitating the rate and yield of desired products. It should be noted that most transition metals already possess catalytic properties in their bulk state; a decrease in particle size to a nanometer regime would result in the enhancement of the existing applications, due to features such as large specific surface areas [23].

1.1.4. Methods for preparing nanoparticles

There are various methods reported in literature for preparing nanoparticles (Figure 1.5). The important task in the field of nanotechnology is to synthesize high quality nanoparticles, because of their technical and fundamental significances. There are three distinctive approaches for the synthesis and functionalization of nanoparticles, namely: bottom-up approach, top-down approach, and template-directed approach [24-25].

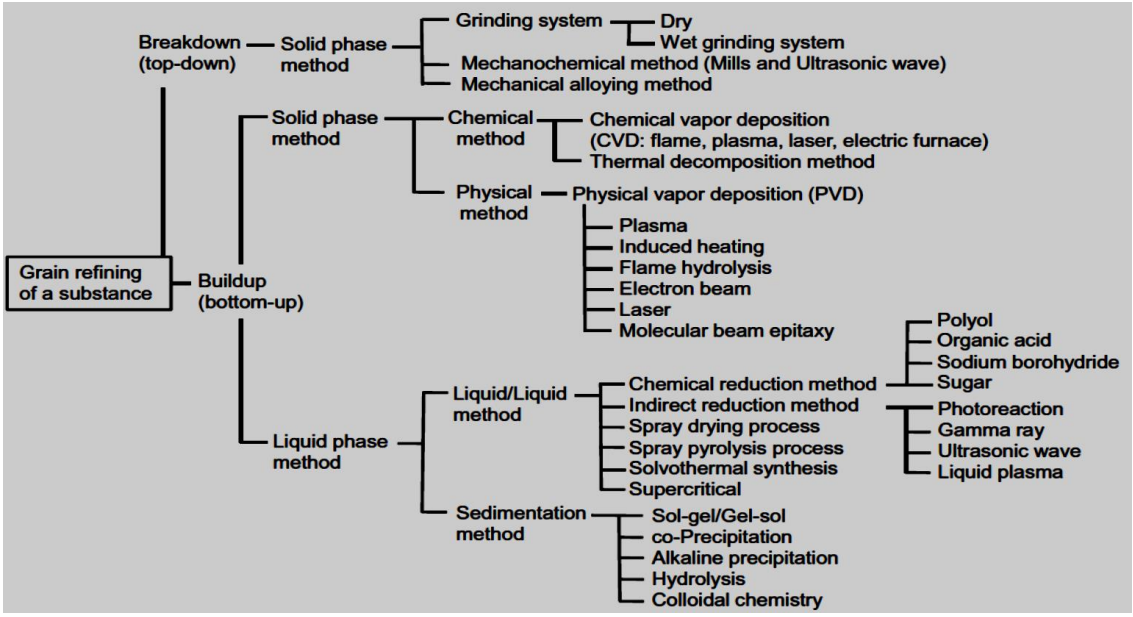

Figure 1.5: Synthetic protocols used to fabricate nanoparticles.

1.1.4.1. Bottom-up approach

This approach is progressively applied to fabricate nanostructures on the relatively smaller scale, as well as more complex structural design. It also involves the invention of structures from smaller units, thus using the properties they have in order to make their self-assembly in the desired manner (Figure 1.6). This is a more affluent approach in that it allows a better control of the nanometric state, i.e. homogeneity, particle sizes and monodispersed granulometric distribution of nanomaterial-based products. This approach generally involves the conversion of multiple precursors *via* a definite reaction protocol such as reduction, pyrolysis, inert gas condensation, solvothermal reaction, sol-gel fabrication, and decomposition or hydrolysis into nuclei that subsequently grow into monodispersed nanoparticles.

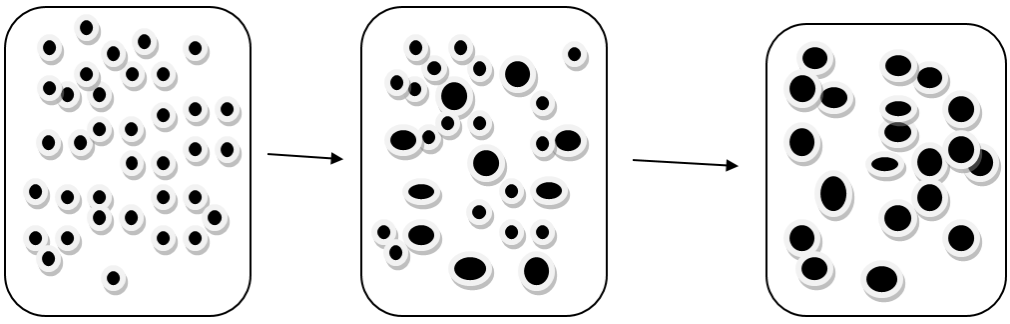

Figure 1.6: Bottom-up approach for synthesizing nanoparticles [25].

1.1.4.2. Top-down approach

This approach is a break-down of bulk material into relatively smaller particles (Figure 1.7). It is capable of higher-volume fabrication through non-sophisticated protocols. The protocols can either be mechanically or chemically-mediated. The most common process involves adding the bulk material in a hot coordinating solvent, where it dissolves/suspended and sheared to produce colloidal particles.

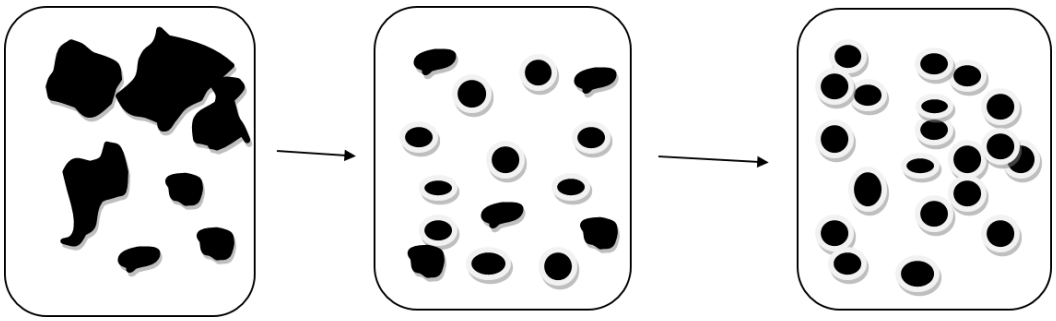

Figure 1.7: Top-down approach for synthesizing nanoparticles [25].

1.1.4.3. Template-directed approach

Under this approach, the colloidal particles which are obtained either mechanically or chemically, are coated with desired materials to afford functionalized nanocomposites (Figure 1.8). The colloidal particles can also be grown on substrates, thus assuming shape of their template.

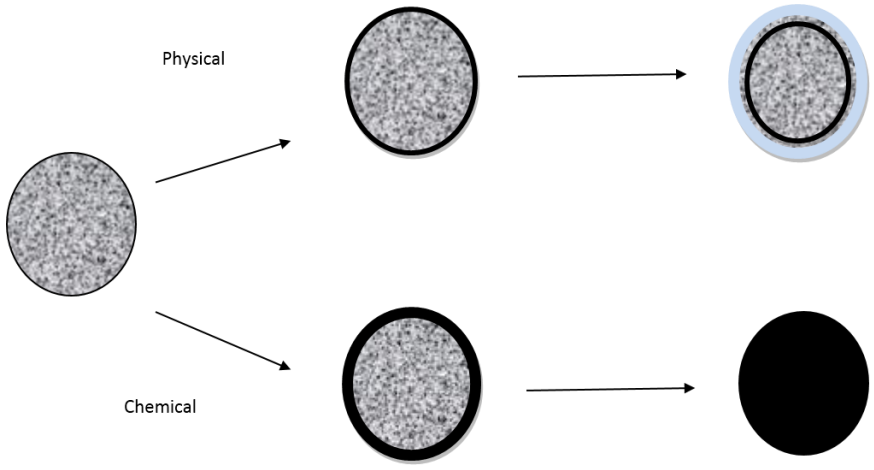

Figure 1.8: Template-directed approach for synthesizing nanoparticles [25].

1.1.4.4. Single-source precursor (SSPs) method

The use of single source molecular precursors which are basically metal-ligand complexes containing desired pre-formed bonds, has proven to be an efficient route for producing pure, high-quality nanoparticles. Common practice involves subjection of the SSPs to thermal decomposition in the presence of a coordinating solvent, thus promoting the crystallinity and passivation of the as-prepared nanoparticles.

Trindade and O'Brien investigated the use of cadmium(II) dithio- and diselenocarbamate complexes as SSPs for the preparation of TOPO-capped CdS (II-VI) nanomaterials [26]. Research groups of Revaprasadu and O'Brien have extensively reported the synthesis of many metal chalcogenides nanoparticles through exploitation of complexes of thioureas, xanthates and thiosemicarbazides [27-31]. The resulting nanoparticles displayed both isotropic and anisotropic morphologies.

Revaprasadu and co-workers pioneered the use of heterocyclic piperidine and tetrahydroquinoline dithiocarbamate complexes as SSPs to synthesize metal sulfide nanoparticles [32-40]. There has been a trend from using these complexes to synthesize nanoparticles which includes the study of their properties and morphologies by the effect of varying the reaction parameters. Interests in this SSPs method shifted to the control of particle shape and size in the quantum confinement range, since the desired electronic properties of the nanomaterials are dependent on these parameters. For example, Nyamen *et al* used Zn (Figure 1.9) [32], Cd [33] and Pb [34] as metal center in the complexes with the variation of other parameters (such as temperatures and capping agents) to control sizes and shapes of the nanoparticles. These variation of parameters also influences the optical properties of the materials. Several other heterocyclic metal complexes have also been used to synthesize nanoparticles by greener solvents such as castor oil, ricinoleic acid and other capping agents which influences the phase and morphological transformation of the nanoparticles depending on the varying conditions [35-37].

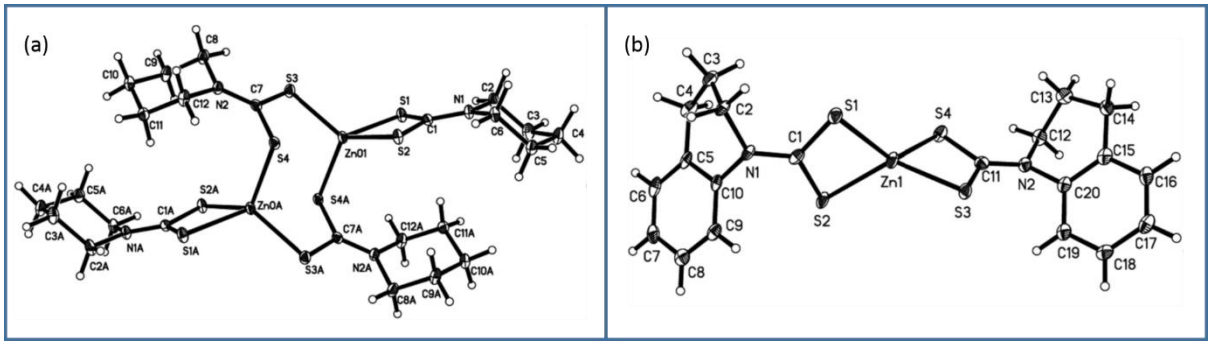

Figure 1.9: X-ray structures for Zn(II) complexes of (a) heterocyclic piperidine and (b) tetrahydroquinoline dithiocarbamates [32].

The advantages of using single source precursors are summarized below [41];

- Non-volatile precursors can be used, which offer little-to-none purification of the nanomaterial produced; the opposite is observed when toxic and/or pyrophoric volatile precursors are used.
- Some II-VI and Ill-V nanoparticles are air and moisture sensitive. However, the corresponding SSPs can be made stable through chemical functionalization, thus, allowing easy storage and longer shelf life.
- Low temperature decomposition routes are possible.
- Despite theoretical model predictions, unanticipated optical and chemical properties of the as-prepared nanoparticles would be observed through this synthetic route. The nature of such results would be of novel origin, or of significant importance in appropriate applications.

Figure 1.10 shows a scheme of various stages of nanoparticle growth using a SSP method [42]. This one-pot synthetic route is consistent with the LaMer mechanism [43, 44] in the formation process of nanoparticles, where the initial rapid burst nucleation occurs during the injection of the precursor in a pot. The controlled growth of the nuclei from stage (II) to stage (III) is caused by the Ostwald ripening process where larger particles grow at the expenses of smaller particles [45]

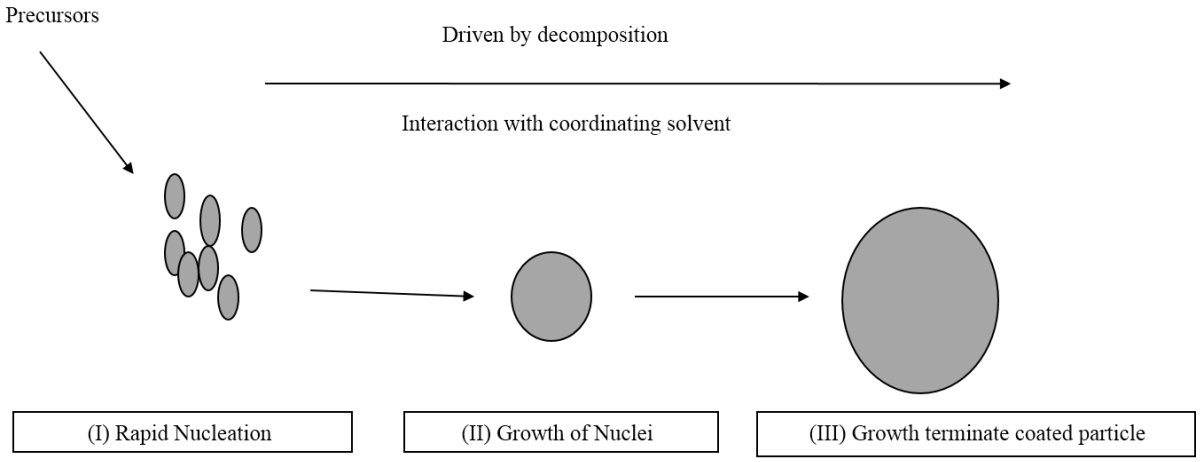

Figure 1.10: Scheme for nanoparticle growth using the SSP method [42].

PART II 1.2. INTRODUCTION

Contents

Since the 19th century, coordination chemistry has been a challenge to inorganic chemistry researchers. It is a multidisciplinary field which incorporates real areas such as analytical chemistry, metallurgy, material science, medicinal chemistry and industrial chemistry. Today, the stereochemistry of coordination compounds is a major interests to coordination chemists, due to the ease of preparation. A good example of such compounds is Schiff base compounds, which have played a crucial role in the development and advancement of coordination chemistry [46-49]. These Schiff bases have been synthesized and used as chelating ligands because they are potentially capable of forming stable complexes with metal ions [50, 51].

Schiff base metal complexes have been widely studied due to their attractive chemical and physical properties, which enable exploitation in a variety of applications in several scientific areas. They have been widely used in pigments and dyes [52], emulsions [53], polymers [54], stabilizers [55], oils [56], agents [57, 58] and liquid crystal display composition [59, 60]. They have also been used in biological entities as antibacterial [61], anticancer, antiviral [62], antifungal [63, 64], antitumor [65, 66], insecticides [67], antihelmintic [68], antiemetic [69] and herbicidal agents [70].

They serve as models for biologically-important species and find applications in biomimetic catalytic reactions [71]. Schiff base complexes of cobalt have been reported in catalyzing ring opening polymerization of cycloalkenes at low temperature and provide a control on the molecular weight of the polymers [72, 73], without any side reaction taking

place. The ring opening of larger cycloalkanes is usually a difficult process which Schiff base complexes of cobalt (II) can efficiently catalyze with significant enantioselectivity [74]. The corrosion inhibition activity of Schiff bases have extensively been studied and reported as well [75-77].

1.2.1. Schiff bases

Schiff bases are compounds named after a German scientist, Hugo Schiff, in 1864 [47]. These compounds, generally, are formed by the condensation reaction of primary amines with carbonyl-functionalized compounds such as aldehydes and ketones, using low alkyl-chained alcohols as a solvent. They are usually identified easily through the carbon nitrogen double bond (C=N). Cozzi [78] stated that the active and well-made Schiff bases are considered as privileged ligands containing the azomethine group (-HC=N-). The general compound formula for Schiff bases is $R_1R_2C{=}NR_3$, where R_1 is an aryl group, R_2 is a hydrogen atom and R_3 is either an alkyl or aryl group [79]. Nevertheless, typically compounds where R_3 is an alkyl or aryl group and R_2 is an alkyl or aromatic group are also considered as Schiff bases.

Schiff bases that contain aryl substituents are considerably more stable, thus making aryl aldehydes and ketones as the preferred starting materials [80, 81]. The opposite is usually observed from aliphatic Schiff base compounds, in addition to further reacting to afford polymerized compounds [82, 83]. The common Schiff bases are crystalline and feebly basic in nature. Those which are prepared from aromatic amines are known as anils.

The azomethine group of Schiff bases has a tendency to donate the lone pair of electrons present in a sp^2-hybridised orbital of nitrogen atom, thus facilitating complexation with transition metals, in an effortless manner. Another feature which makes Schiff bases attractive, is the ease of functionalization, which would result in countless possibilities on preparing new classes [84-91].

In general, Schiff bases with ketones are formed less readily than those from aldehydes starting materials, due to steric hindrance in the active site. Additionally, the extra carbon of ketone donates electron density to the azomethine carbon, and therefore it makes a ketone less electrophilic compared to an aldehyde. The ligands can exhibit polydentate coordination features, depending on the potential donor sites available in their structural skeleton (Figure 1.11). Coordinating possibilities can also be enhanced by incorporating

moieties which contain other more electronegative donor atoms such as oxygen and sulfur. In enzyme catalysis, Schiff bases are preferred because they:

- Retain the oxidation state of the carbonyl group.
- Form a covalent bond to the substrate, in order for the substrate not to diffuse away during the course of the reaction.
- Act as electron sinks and sources for further chemistry.

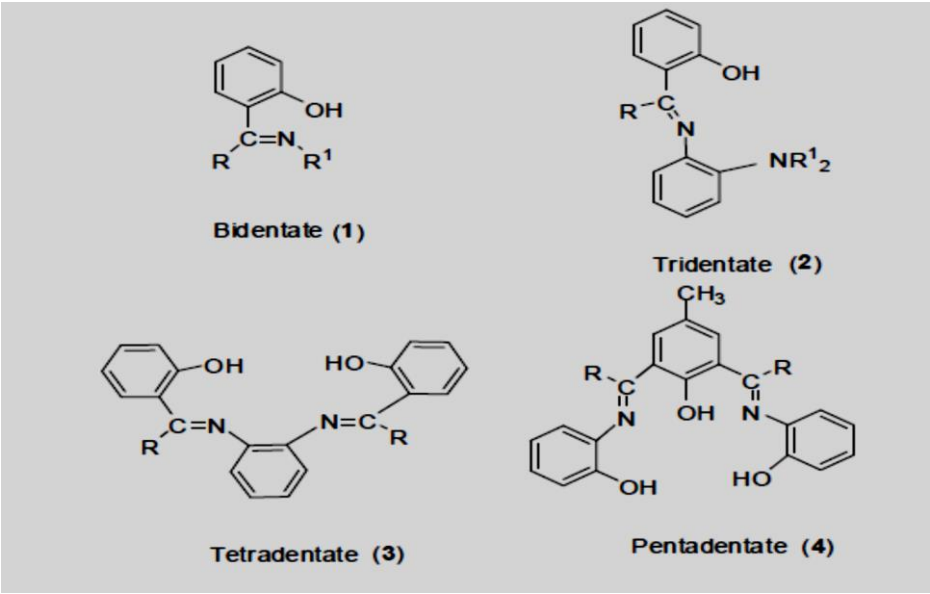

Figure 1.11: Potential polydentate coordination features from Schiff base compounds.

1.2.2. Biological importance of Schiff bases

Schiff bases derived from aromatic amines and aromatic aldehydes have been widely used in many fields of applications, e.g., biological, inorganic and analytical chemistry, and in drug synthesis [92, 93]. Various Schiff bases are well known to be medicinal and are used to create medicinal compounds [94-100]. Their biological importance have been reported for many activities such as antitumor, antimicrobial [101], antifungal [102], anti-inflammatory, anticonvulsant and anti HIV activities [103, 104]. Chelation with metal ions can either enhance or inhibit these properties [105-107].

Schiff bases are also important intermediates in several of enzymatic reactions involving interaction of an enzyme with the amino group of the substrate, usually carbonyl group of the substrate (i.e. lysine residue) [108, 109]. They play a significant role in

transamination reactions on enzymic catalysis (commonly known as transaminases), which occurs in mitochondria and cytosol of eukaryotic cells [110]. Schiff bases derived from pyridoxal, the active form of vitamin B6, and amino acids are extensively studied and considered as very important ligands from a biological point of view [111-115].

Metal complexes of Schiff bases are increasingly important for their biochemical and antimicrobial activities. They show greater activity in drugs, than free organic ligands. The Schiff base metal complexes that have oxygen and nitrogen donor atoms are sensitive to molecular environment, and they possess extraordinary structural lability [116-120].

1.2.3. Schiff base metal complexes

For the metal to coordinate, nitrogen and sulfur atoms play a role at the active sites of numerous metallobiomolecules [121]. There are varieties of pathways in which they bond to metal ions, enabling applications such as biomimetic catalytic reactions. It is well recognized that the presence of metal ions bonded to biologically active compounds may improve their activities [121-124]. The transition metal complexes were investigated on the interactions of DNA with it, which lead to the design of relatively cheap and highly efficient drugs, and also the development of sensitive probes for DNA [125, 126]. Holm *et al.* [85] published a review which documents a lot of metal complexes of Schiff bases, which are derived from the salicylaldehyde starting material.

1.2.4. Application of Schiff base metal complexes

1.2.4.1. Catalysts

Schiff base complexes catalyze a huge number of organic reactions, as well as oxygen transfer agents to organic compounds [127-129]. They are mostly exploited in hydrolysis, aldol condensation, redox and elimination catalytic reactions.

Salen complexes are well known classes of Schiff base complexes; they transfer oxygen atom to an alkene forming epoxide. Schiff base complexes of Co(II) form super-oxo complexes by reacting with dioxygen. This phenomenon was studied and concluded by Calvin and Martell [130]. Nishinaga *et al.* [131] reported the catalysis of Co(II) Schiff base complexes leading to the corresponding p-quinols in which peroxy-p-quinolato was found as

an intermediate. Van Dort and Geursen were the first to use Co(II)salen on oxidative catalysis of phenols to the equivalent quinines [132].

Phosphene-based ligand complexes are generally used to catalyze Heck reaction, but Schiff base complexes have recently been used as alternative catalysts, simply because they are easily prepared and they showed high catalytic activity than the commercially used phosphine-based complexes [133, 134]. Apart from Co(II), other metals such as Fe(II), Ni(II), and Cu(II) have been complexed to Schiff base ligands.

1.2.5. History and occurrence of Cobalt

Cobalt (Co) is a hard, lustrous, silver-gray metal of atomic number 27, and has an electron configuration of [Ar] $4s^2$ $3d^7$. It exists in six oxidation states: 0, +1, +2, +3, +4, and +5, although the most common oxidation states are +2 and +3. The word 'cobalt' was named in the 16^{th} century after a German term *kobold*, which means goblin or evil spirit. *Kobold* was used to describe cobalt ores which being smelted for their silver content, it would produce poisonous arsenic trioxide fumes. Prior to this, around 1450 B.C., Co compounds were used for applications in blue dyes for pottery, glazes and glass.

Georg Brandt, a Swedish chemist, achieved the first isolation of Co from copper ore in 1735, and confirmed that the blue pigment arose from Co, not arsenic or bismuth as all chemists originally believed. Other natural sources of Co include: cobaltite, erythrite, glaucodot and skutterudite mineral ores [135-141]. Then in the 20^{th} century, the Co metal rarely receives attention shortly after the 1900s when the American automotive entrepreneur, Elwood Haynes, developed a new corrosion resistant Co-containing alloy, which he referred to as stellite. Patented in 1907, stellite alloys contain high cobalt and chromium contents and are completely non-magnetic [142-144].

PART III 1.3.

Contents

1.3.1. Scope of the work

The proposed work focuses on synthesizing and characterizing a series of novel, symmetrical and unsymmetrical tetradentate Schiff base compounds derived from the condensation of carbonyl-containing compounds with aromatic diamines. The resulting Schiff bases are complexed to Co(II), and then subsequently utilized as single source molecular precursors towards the preparation of organically-capped Co metal nanoparticles.

1.3.2. Aims and Objectives of the Study

The main aim of this work is the preparation of self-assembled monodispersed cobalt nanoparticles by thermal decomposition of cobalt(II) Schiff base complexes, in the presence of organic surfactants, namely: oleylamine, 1-dodecanethiol and hexadecylamine.

The objectives of this work are to:

(a) Synthesize and characterize a series of symmetrical and unsymmetrical Schiff base compounds.
(b) Coordinate the preformed ligands to cobalt (II) to form the corresponding cobalt (II) Schiff base complexes.
(c) Establish the purity of both the Schiff bases and the cobalt (II) complexes.

(d) Prepare uniformly sized, monodispersed, and size-tunable cobalt and cobalt sulfide nanoparticles using the thermal decomposition method in the presence of organic surfactants.

(e) Investigate the morphology, crystal structure and magnetic properties of the cobalt and cobalt sulfide nanoparticles.

1.3.3. Outline of the dissertation

This thesis consist of four chapters which are briefly summarized below:

Chapter One: Introduction and literature survey

Chapter one is divided into three parts, **Part I** presents the general theory of nanotechnology and the basic principles of metal nanoparticles, which discusses the characteristic properties and their chemically synthesized protocols. Fundamental routes of nanomaterials are described. **Part II** explains the theory of Schiff bases, in particular their properties and reviews in Schiff base complex. The history of the element cobalt is also briefly reviewed. **Part III** includes the context, scope and the objectives of the work which are outlined.

Chapter Two: Synthesis of Schiff base ligands and cobalt Schiff base complexes

Chapter two discusses the synthesis of the symmetrical and unsymmetrical Schiff bases and their cobalt(II) complexes. The aim of this chapter is to focus more on the synthesis of new Schiff base and the stereochemistry of four-coordinate chelate complexes using reported routes. The ligands and complexes are characterized using several techniques.

Chapter Three: Synthesis of cobalt nanoparticles by thermal decomposition of Schiff base complexes

Chapter three describes the synthesis of magnetic nanomaterials by the synthetic route reported in the group. The aim of this chapter is to synthesize cobalt nanoparticles only but with the expectations of producing cobalt oxide nanoparticles because of the two oxygen in the Schiff base coordinated to the metal center, and the significant impact of changing parameters such as time and temperatures.

Chapter Four: Cobalt Schiff base complexes: Single source precursor for cobalt sulfide (Co_9S_8 and Co_3S_4) nanoparticles

The aim of chapter four is to synthesize cobalt sulfide nanoparticles by the thermal decomposition of cobalt Schiff base complexes in a presence of the surfactant containing sulfur. 1-Dodecanethiol plays a major role as a sulfur source and stabilizing agent. Characterization techniques are described to show the potential of the capping agent as sulfur source and the morphology of the synthesized cobalt sulfide nanoparticles.

Chapter Five: Conclusion and future prospects

A conclusion and future prospects are given in Chapter 5.

1.4. References

1. C. Kumar; Nanomaterials for Medical Diagnosis and Therapy, Wiley-VCH; 1(2007) 51- 53, 310-311, 597-559.
2. C. N. R. Rao, A. Muller, A. K. Cheetham; The Chemistry of Nanomaterials: Synthesis, Properties and Applications Volume 1, Wiley-VCH, Weinheim (2004).
3. R. W. Siegel; Annu. Rev. Mater. Sci., 21 (1991) 559.
4. R. W. Siegel; Springer Ser. Mater. Sci., (1994) 65.
5. N. Kobayasi; Nanotechnology, Japan, (2001); Russia, (2005).
6. A. Gussev; Nanomaterials, nanostructures, nanotechnologies (Fizmatlit, Moscow, (2005).
7. A. Gurav, T. Kodas, T. Pluym, Y. Xiong; Aerosol Sci. Technol., 19 (1993) 411.
8. S. Bedanta, A. Barman, W. Kleemann, O. Petracic, and T. Seki; J. Nanomater., (2013) 22.
9. T. Hyeon; Chem. Commun., (2003) 927.
10. A. R. Tao, S. Habas, P. Yang; Small, 4 (3) (2008) 310.
11. J. Robin, J. White, L. Vitaly, W. B. James, H. C. James; Int. J. Mol. Sci., 12 (2011) 5782.
12. A. C. Templeton, W. P. Wuelfing, R. W. Murray; Acc. Chem. Res., 33 (2000) 27.
13. M. C. Daniel, D. Astruc; Chem. Rev., 104 (2004) 293.
14. R. J. White, R. Luque, V. L. Budarin, J. H. Clark, D. J. Macquarrie; Chem. Soc. Rev., 38 (2009) 481.
15. R.W. Wood; Proc. Phys. Soc., London, 18 (1902) 269.
16. R.W. Wood; Philos. Mag., 4 (1902) 396.
17. R.W. Wood; Philys. Mag., 23 (1912) 310.
18. L. Rayleigh; Proc. R. Soc., London Ser. A, 79 (1907) 399.
19. U. J. Fano; Opt. Soc. Am., 31 (1941) 213.
20. A. Z. Otto; Phys., 216 (1968) 398.
21. E. Kretschmann, H. Z. Raether; Naturforsch. Teil A, 23 (1968) 2135.
22. J. M. Campelo; Chem. Sus. Chem., (2009) 2.
23. N. C. Bigall, A. Eychmuller; Phil. Trans. R. Soc. A, 368 (2010) 1385.
24. M. Shimomura, T. Sawadaishi; Curr. Opin. Colloid Interface Sci., 6 (2001) 11.

25. U. Jeong, Y. Wang, M. Ibisate, Y. Xia; Adv. Funct. Mater., 15 (2005) 1907.

26. T. Trindade, P. O'Brien; Adv. Mater., 8 (1996) 161.

27. N. Revaprasadu, M. A. Malik, P. O'Brien, M. M. Zulu, G. Wekefield; J. Mater. Chem., 8 (1998) 1885.

28. N. Revaprasadu, M.A. Malik, P. O'Brien; J. Mater. Res., 14 (1999) 3237.

29. M. A. Malik, P. O'Brien, S. N. Mlondo, N. Revaprasadu; Mater. Res. Soc. Symp. Proc., Z7 (2005) 13.

30. P. S. Nair, T. Radhakrishnan, N. Revaprasadu, G. A. Kolawole, P. O'Brien; J. Mater. Chem., 9 (2001) 1555.

31. P. S. Nair, T. Radhakrishnan, N. Revaprasadu, P. O'Brien; Mater. Sci. Technol., 12 (2002) 1.

32. L. D. Nyamen, A. A. Nejo, V. S. R. Pullabhotla, P. T. Ndifon, M. A Malik, J. Akhtar, P. O'Brien, N. Revaprasadu; Polyhedron 67 (2014) 129.

33. L. D. Nyamen, V. S. R. Pullabhotla, A. A. Nejo, P. T. Ndifon, N. Revaprasadu; New J. Chem., 35 (2011) 1133.

34. L. D. Nyamen, V. S. R. Pullabhotla, A. A. Nejo, P. T. Ndifon, J. H. Warner, N. Revaprasadu; Dalton Trans., 41 (2012) 8297.

35. G. B. Shombe, E. B. Mabofu, S. Mlowe, N. Revaprasadu; Mater. Sci. Semicond. Process, 43 (2016) 230.

36. G. B. Shombe, E. B. Mabofu, S. Mlowe, N. Revaprasadu; Mater.lett.,185 (2016) 17-20.

37. J. W. M. Kyobe, E. B. Mabofu, Y. M. M. Makame, S. Mlowe, N. Revaprasadu; Int. Nano. Lett., 6 (2016) 235.

38. C. Gervas, S. Mlowe, M. P. Akerman, I. Ezekiel, T. Moyo, N. Revaprasadu; Polyhedron, 122 (2017) 16.

39. S. Mlowe, D. J. Lewis, M. A. Malik, J. Raftery, E. B. Mabofu, P. O'Brien, N. Revaprasadu; New J. Chem., 38 (2014) 6073.

40. S. Mlowe, S. S. Garje, T. Moyo, N. Revaprasadu; MRS Adv., 1 (2016) 235.

41. L. N. Pickett, P. O'Brien; Chem. Rec., 1 (2001) 470.

42. M. A. Malik, P. O'Brien; Relat. Elem., 180 (2005) 689.

43. V. K. La Mer, R. H. Dinegar; J. Am. Chem. Soc., 72 (1950) 4847.

44. V. K. La Mer; Ind. Eng. Chem., 44 (1952) 1270.

45. P. Taylor; Adv. Colloid Interface Sci., 75 (1998) 107.

46. C. Ettling; Ann. Chem. Pharm., 35 (1840) 241.

47. H. Schiff; Ann. Suppl., 3 (1864) 343.

48. J. E. Huheey, E. A. Keiter, R. L. Keiter; Harper Collins College Publishers, New York 4 (1993).

49. R. H. Holm; J. Am. Chem. Soc., 82 (1960) 5632.

50. C. P. Johnson, J. L. Atwood, J. W. Steed, C. B. Bauer, R. D. Rogers; Inorg. Chem., 35 (1996) 2602.

51. N. Alizadeh, S. Ershad, H. Naeimi, H. Sharghi, M. Shamsipur; Pol. J. Chem., 73 (1999) 915.

52. K. Taramura, J. Nakano, S. Lot; Chem. Abstr., 71 (1979) 114093.

53. R. B. Zhurin, D. L. Rodichera, B. A. Chartorishi; Zh. Obsch. Khim., 33 (1963) 3360.

54. F. C. McCoy, E. C. Knaloy; Chem. Abstr., 66 (1967) 4734.

55. H. A. Cyba; Chem. Abstr., 68 (1968) 6364.

56. T. Kimura; Chem. Abstr., 79 (1973) 146264n.

57. A. G. Farabenfabrikon Bayer; Ger. 1, 108 (1956) 659.

58. A. Badische, A. G.Soda; Fabric Brit. 1, 122 (1969) 938.

59. J. J. Moraianoos, S. P. Aams; Adams U. S. Patent, 3 (1976) 960.

60. W. Costain, W. H. Terry; Chem Abstr., 85 (1976) 147255a.

61. Y. A. Attia; Chem Abstr., 87 (1977) 185326y.

62. N. S. Kozolv, U. D. Pak, V. V. Mashevsku; Pharm. Ah., 7 (1973) 15.

63. G. Cavalline, E. Massarani, D. F. Nardi, Tenconi, L. Mauri; Chem Abstr., 62 (1965) 1590.

64. B. Das, M. Patra, P. K. Mahapatra; J. Ind. Chem. Soc., 60 (1983) 772.

65. Goyal Sudha, Keemti Lal; J. Ind. Chem. Soc., 66 (1989) 477.

66. T. D. Chaudhari, S. S. Salensis; Bull. Hoffkins Inst., 4 (1976) 85.

67. E. M. Hodnett, P. D. Money; J. Med. Chem., 12 (1970) 786.

68. A. D. Gutmann; Chem Abstr., 87 (1977) 6192.

69. E. Profit, E. Hoegel; East Ger. Pat., 97 (1973); Chem Abstr., 80 (1974) 26913.

70. K. Singh, M. S. Barwa, P. Tyagi; Eur. J. Med. Chem., 42 (2007) 3.

71. A. A. Nejo, G. A. Kolawole, A. R. Opoku, J. Wolowska, P. O. Brien; Inorg. Chim. Acta, 362 (2009) 3993.

72. J. P. Claverie, R. Soula; Prog. Polym.Sci., 28 (2003) 619.

73. T. M. Trnka, R. H. Grubbs; Acc. Chem. Res., 34 (2001) 18.

74. E. N. Jacobsen, F. Kakiuchi, R. G. Konsler, J. F. Larrow, M. Tokunaga; Tetrahedron Lett., 38 (1997) 773.

75. M. A. Houji, S. Chen Niu Lini, S. Shang, S. Li, S. Zaho, Q. Zhenlan; J. Electrochem. Soc., 5 (2001) 148.

76. N. K. Mehtal, V. S. Agrawal; Int. Corros. Congr. Proc., 13 (1996).

77. S. L. Li, S. Chen, S. Lei, H. Ma, Y Rui; Corros. Sci., 41 (1999) 1273.

78. P. G. Cozzi; Chem. Soc. Rev., 33 (2004) 410.

79. T. P. Yoon, E. N. Jacobsen; Science, 299 (2003) 1691.

80. H. Tazoki, K. Miyano; J. Chem. Soc., (1959) 9769.

81. C. M. Brewster; J. Am. Chem. Soc., 46 (1924) 2463.

82. K. N. Campbell, H. Sommers, B. K. Campbell; J. Am. Chem. Soc., 66 (1944) 82.

83. J. Hine, C. Y. Yeh; J. Am. Chem. Soc., 89 (1967) 2669.

84. B. De Clercq, F. Verpoort; J. Mol. Catal. A: Chem., 180 (2002) 67.

85. R. H. Holm, G. W. Everett, A. Chakraborthy; Prog. Inorg. Chem., 7 (1966) 83.

86. S. Yamada; Coord. Chem. Rev., 1 (1966) 415; 2(1967) 82.

87. J. F. Geldard, F. Lions; Inorg. Chem., 4 (1965) 414.

88. S. Adsule, V. Barve, D. Chen, F. Ahmed, Q. P. Dou, S. Padhye, F. H. Sarkar; J. Med. Chem., 49 (2006) 7242.

89. X. H. Bu, M. L. Tong, Y. B. Xie, J. R. Li, H. C. Chang, S. Kitagawa, J. Ribas; Inorg. Chem., 44 (2005) 9837.

90. C. G. Zhang, D. Wu, C. X. Zhao, J. Sun, X. F. Kong; Transition Met. Chem., 24 (1999) 718.

91. E. Tas, M. Aslanoglu, M. Ulusoy, M. Guler; Pol. J. Chem., 78 (2004) 903.

92. Z. Cimerman, S. Miljanic, N. Galic; Croatica Chemica Acta, 73 (1) (2000) 81.

93. A. Elmali, M. Kabak, Y. Elerman; J. Mol. Struct., 477 (2000) 151.

94. S. K. Chakraborti, B. Kumar; J. Indian Chem. Soc., (1973) 137.

95. S. Rao, AS. Mittra; J. Indian Chem., Soc. (1978) 420.

96. S. A. Khan, A. A. Siddiqui, S. Bhatt; Asian J. Chem., 14 (2002) 1117.

97. J. Patole, D. Shingnapurkar, S. Padhye, C. Ratledge; Bioorg. Med. Chem. Lett., 16 (2006) 1514.

98. V. T. Dao, M. K. Dowd, M. T. Martin, C. Gaspard, M. Mayer, R. J. Michelot; European J. Med. Chem., 39 (2004) 619.

99. A. Khan, S. Sarkar, D. Sarkar; Int. J. Antimicrob. Agents, 32 (2008) 40.

100. M. S. Iqbal, A. H. Khan, B. A. Loothar, I. H. Bukhari; Med. Chem. Res., 18 (2009) 31-42

101. M. Abdul-Gawad, Y. M. Issa, S. M. Abd-Alhamid; Egypt J. Pharm. Sci. 34 (1993) 219.

102. K. Sahu, R. K. Behera, R. C. Pathaik, A. Nayak, G. B. Behera; Indian J. Chem., 18B (1979) 557.

103. S. N. Pandeya, D. Sriram, G. Nath, E. De Clercq; Pharm. Acta Helv., 74 (1999) 11.

104. M. K. Taylor, J. Reglinski, D. Wallace; Polyhedron, 23 (2004) 3201.

105. P. G. Kulkarni, G. B. Avaji, Bagihalli, S. A. Patil, P. S. Badami. J. Coord. Chem., 62 (2009) 481-492

106. G. Puthilibai, S. Vasudevan, S. K. Rani, G. Rajagopal; Spectrochim. Acta, 72 (2009) 796.

107. N. Chitrapriya, V. Mahalingam, L. C. Channels, M. Zeller, F. R. Fronczek, K. Natarajan. Inorg. Chim. Acta, 361 (2008) 2841.

108. H. R. Mahler, E. H. Cordes; Bio. Chem., New York. 1 (1971).

109. A. L. Lehlinger, Principles of biochemistry, Worth, New York, (1975).

110. G. H. Schmid, Organic Chemistry, New York, (1996).

111. J. S. Casas, A. Castineiras, F. Condori, M. D. Couce, U. Russo, A. Sanchez, R. I Seoane, J. Sordo, J. M. Varela; Polyhedron, 22 (2003) 53.

112. S. Naskar, S. Naskar, H. M. Figgie, W. S. Sheldrick, S. K. Chattopadhyay; Polyhedron 29 (2010) 493.

113. I. I. Mathews, H. Manohar; J. Inorg. Biochem., 46 (1992) 259.

114. P. A. M. Hughes, D. N. Raine; Clin. Chim. Acta, 14 (1966) 399.

115. N. Al-Awadi, M. S. El-Ezaby, H. Abu-Soud; Inorg. Chem. Acta, 67 (1982) 131.

116. E. Kimura, R. Machida, M. Kochima; J. Am. Chem. Soc., 106 (1984) 5497.

117. J. W. Pyrz, A. I. Roe, L. J. Stem, J. R. Que; J. Am. Chem. Soc., 107 (1985) 614.

118. M. Turner, B. Erdogan, H. Koksal, S. Serin, M. Y. Nutku; Synth. React. Inorg. Met. Org. Chem., 28 (1998) 529.

119. W. Zishen, L. Zhiping, Y. Zhenhuan; Trans. Met. Chem., 18 (1993) 291.

120. J. Chakraborty, R. N. Patel; J. Ind. Chem. Soc., 73 (1996) 191.

121. D. H. Brown, W.E. Smith; Chapmann and Hall, London, (1990).

122. M. B. Ferrari, S. Capacchi, G. Pelosi, G. Reffo, P. Tarasconi, R. Albertini, S. Pinelli, P. Lunghi; Inorg. Chim. Acta, 286 (1999) 134.

123. E. Canpolat, M. Kaya; J. Coord. Chem., 57 (2004) 1217.

124. M. Yildiz, B. Dulger, S.Y. Koyuncu, B.M. Yapici; J. Indian Chem. Soc., 81 (2004) 7.

125. C. Liu, M. Wang, T. Zhang, H. Sun; Coord. Chem. Rev., 248 (2004) 147.

126. D. S. Sigman, A. Mazumder, D. M. Perrin; Chem. Rev., 93 (1993) 2295.

127. T. C. Siddal, N. Miyara; J. Chem. Soc. Chem. Commun., (1983) 1185.

128. E. G. Samsel, K. Srinivasan; J.Am. Chem. Soc., (1983) 107.

129. V. Bansel, P. K. Sharma, K. K. Banerji; Ind. J. Chem., 39 (2000) 654.

130. M. Calvin, A. E. Martell; Prentica Hall, Inc. New Jersey, (1959) 254.

131. A. Nishinaga, H. Tomita, T. Matsuura; Tetrahedron Lett., 21 (1980) 4849.

132. H. M. Van Dort, H. J. Geusen; Academic Press, New York. (1981).

133. A. Kumar, M. Agarwal, A. K. Singh; Polyhedron, 27 (2008) 485.

134. S. Iyer, G. M. Kulkarni, C. Ramesh; Tetrahedron, 60 (2004) 2163.

135. D. A. Ptitsyn,; V. M. Chechetkin; Sov. Astron. Lett., 6 (1980) 61.

136. F. P. Kerr; Amer. Miner., 30 (1945) 483.

137. A. N. Buckley; Australian J. Chem., 40 (2) (1987) 231.

138. R. Young; Geochim. Cosmochim. Acta, 13 (1957) 28.

139. B. Shedd, Kim; "Mineral Yearbook 2006: Cobalt". United States Geological Survey. Retrieved 2008-10-26. Accessed 2013-04-01.

140. B. Shedd, Kim; "Commodity Report 2008: Cobalt". United States Geological Survey. Retrieved 2008-10-26. Accessed 2013-04-01.

141. A. F. Holleman, E. Wiberg, , N. Wiberg; Lehrbuch der Anorganischen Chemie, 102nd ed. (in German). de Gruyter, (2007) 1146.

142. http://www.thenaturalrecoveryplan.com/articles/Cobalt-Toxicity.html accessed on 10 April 2013.

143. A. Linna, P. Oksa, P. Palmroos, P. Roto, P. Laippala, J. Uitti; Am. J. Ind. Med., 44 (2003) 124.

144. D. Anard, M. Kirsch-Volders, A. Elhajouji, K. Belpaeme, D. Lison; Carcinogenesis 18 (1997) 177.

Chapter 2

Synthesis of Schiff Base Ligands and Cobalt Schiff Base Complexes

Chapter 2

Synthesis of Schiff Base Ligands and Cobalt Schiff Base Complexes

2.1. INTRODUCTION

Contents

2.1. Introduction

Tetradentate Schiff base complexes of cobalt have been studied by many researchers [1-3]. Cobalt (II) Schiff-base complexes are used as simplified models mostly in a study of reversible binding of dioxygen in the field of biological and pharmaceutical activities [4-6]. Metal complexes of Schiff bases are attractive and increasingly important for their biochemical and antimicrobial activities as they show greater activity in drugs than free organic ligands. The greatest attention given to transition metal complexes containing O, N and S donor atoms is their microbial activities in biochemistry. The Schiff base metal complexes that have oxygen and nitrogen donors are sensitive to the molecular environment, and possess extraordinary formation structural lability [7-11]. These complexes have been derived from the Schiff-base ligands which have been synthesized and used as chelating ligands because they are potentially capable of forming stable complexes with metal ions [12, 13]. Schiff- bases play an important part in the development of coordination chemistry and they are broadly applied in many areas of science such as analytical chemistry, metallurgy, materials science, medicinal and industrial chemistry [14-17].

This chapter will focus on the synthesis of new symmetrical and unsymmetrical Schiff bases and their cobalt complexes. The characterization techniques will be used for analytical and spectroscopic data that should enable us to propose possible structures with the tetradentate coordination via the azomethine group and the phenolic groups.

2.2. Experimental

2.2.1. Materials

All the reagents and chemicals were of analytical or spectroscopic grade and of used as purchased. The chemicals and solvents used for preparation of Schiff-base ligands and Cobalt Schiff- base complexes purchased from Aldrich-Sigma are 2-hydroxy-1-naphthaldehyde, 3,4-diaminobenzoic acid, , 2-hydroxy-3-methylbenzaldehyde, Cobalt (II) acetate, 4-methyl-*o*-phenylendiamin, 2-hydroxy-5-methoxybenzaldehyde and triethylamine. The solvents that were purchased at Merck include ethanol, methanol and diethylether.

2.2.2. Instrumentation

The Schiff base ligands were characterized by elemental analysis (CHN), ^{1}H NMR spectroscopy to study the proton distribution and Fourier transform infrared spectroscopy (FTIR) to determine the functional groups in the sample.

Cobalt Schiff base complexes were also characterized by elemental analysis, FTIR, thermogravimetric (TGA) for determining the weight loss of the sample and differential scanning calorimetry (DSC) to measure the energy/temperature difference between the substance and the reference material.

2.2.2.1. Fourier Transformation Infrared (FT-IR) Spectroscopy

FT-IR Spectroscopy is widely used to study the chemical bonds in a molecule at the various frequencies, depending on the type of elements and the bonds in a compound. FT-IR deals with vibrations and rotations of the bonds in the molecule. As the frequency of the vibration increases, the ground and excited states start to form a transition between them. The infrared region of the electromagnetic spectrum is from 4000 to 400 cm^{-1} and by the recent development on the infrared absorption spectrum, the pattern acts as a molecular fingerprint [18]. For example, FT-IR spectra at the region (1400-1700 cm-1) provides information about the presence of –CO- and –NH- functional groups.

Infrared spectra were recorded on a Bruker FT-IR tensor 27 spectrophotometer, equipped with a standard ATR crystal cell detector. A small sample (10 mg) of the compounds was analysed in the wavenumber range, 200– 4000 cm^{-1}.

2.2.2.2. Thermogravimetric analysis (TGA) and Differential scanning calorimetry (DSC)

TGA is a technique which is monitored by the mass of the sample against time and temperature, usually linear with time as the temperature increases in a stated atmosphere. This technique is used to study the thermal decomposition of the sample. The data obtained by the instrument will plot a thermal decomposition curve [19] in which mass percent is a function of the temperature. TGA normally uses a solid sample, crystalline and fine powders behave differently. The atmosphere in TGA must be inert in order to control development of gases produced by the sample.

DSC is a thermoanalytical technique that is used to monitor heat effects connected with phase transitions and chemical reactions as a function of temperature. This is most widely used technique in which the difference in energy inputs into a substance and a reference material is measured as a function of temperature while the substance and the reference material are subjected to a controlled temperature program.

A Perkin Elmer Pyris 6 Thermogravimetric analyses (TGA) equipped with a closed perforated ceramic pan were used to determine the composition of the complexes, carried out at 20 °C/min heating at from 30 °C to 800 °C under N_2 gas flow rate 10 mL/min.

2.2.2.3. ^{1}H Nuclear Magnetic Resonance (NMR)

Nuclear Magnetic Resonance (NMR) is an analytical tool that is based on the bulk magnetic properties [20] of the materials which is made up of isotopes, particularly, proton (^{1}H) and other types of isotopes (^{13}C, ^{19}F and ^{29}Si). Pauli [21] proposed the magnetic properties by explaining the hyperfine structure features of atomic spectra. The rules for determining the net spin of a nucleus are as follows: If the number of electrons and protons are both even, the nucleus has no spin; If the number of neutrons plus number protons is odd, the nucleus has a half-integer spin (1/2, 2/2, 5/2 etc); If the number of neutrons and the number of protons are both odd, the nucleus has an integer spin (1, 2, 3 etc).

The ^{1}H NMR spectra of both the Schiff base ligands and metal complexes were obtained using a Bruker Advance III 400 MHz spectrophotometer, equipped with trimethylsilane as an internal standard reference.

2.2.2.4. CHNS/O analyser

CHNS/O analyser is the instrument which is used to determine elements in organic and inorganic materials. The technique of the analyser is to produce the weight percentage of elements in compounds [22].

Elemental (C, H, N) microanalysis provides a high sensitive analysis of a sample's atomic composition, Microanalysis was performed on a Perkin-Elmer automated model 2400 series II CHNS/O analyser.

2.2.3. Synthesis of Schiff base ligands

2.2.3.1. Synthesis of N,N'-bis(1-naphthaldehyde)-4-methylorthophenylenediamine [Ligand (1)]

The Schiff base ligand (**1**) (Figure 2.1a) was prepared by the condensation of 2-hydroxy-1-naphthaldehyde (6.91 g, 40 mmol) with 4-methylorthophenylenediamine (2.47 g, 20 mmol) in ethanol (75 mL, 2:1 molar ratio). The condensation reaction was carried out at 50 ^{o}C for 2 h. The product obtained was filtered hot, dried and preserved in a desiccator.

Yield: 80.4 %; ^{1}H-NMR (400 MHz, DMSO-d_6, δ/ ppm): 15.2 (2H, s, O–H), 9.7 (2H, s, -N=CH), 6.9-8.1 (9H, m, aromatic), 2.4 (3H, s, -CH_3), 8.4-8.7 (6H, s, -OCH_3); IR (ATR, cm^{-1}): 1619 (-C=N stretching of azomethine group), 1329 (-C–O stretching of phenolic group); Anal. Calcd. for $C_{29}H_{22}N_2O_2$: C, 80.91; H, 5.15; N, 6.51. Found: C, 79.83; H, 4.76; N, 6.22.

2.2.3.2. Synthesis of N,N'-bis(5-methoxybenzaldehyde)-4-methylorthophenylenediamine [Ligand (2)]

The Schiff base ligand (**2**) (Figure 2.1b) was prepared by the condensation of 5-methoxybenzaldehyde (2.72 g, 20 mmol) with 4-methylorthophenylenediamine (1.24 g, 10 mmol) in ethanol (75 mL, 2:1 molar ratio). The condensation reaction was carried out at 50 °C for 2 h. The product obtained was filtered hot, dried and preserved in a desiccator.

Yield: 87.5 %; ^{1}H-NMR (400 MHz, DMSO-d_6, δ/ ppm): 12.46 (2H, s, O–H), 8.92 (2H, s, -N=CH), 6.98-7.39 (9H, m, aromatic), 2.57 (3H, s, -CH_3), 3.86 (6H, s, -OCH_3); IR (ATR, cm^{-}

^{1}): 1621 (-C=N stretching of azomethine group), 1334 (-C–O stretching of phenolic group); Anal. Calcd. for $C_{23}H_{22}N_2O_4$: C, 70.75; H, 5.68; N, 7.17. Found: C, 70.51; H, 5.70; N, 6.88.

2.2.3.3. Synthesis of N-(naphthaldehyde)- N'-(3-methylbenzylidene)benzoic acid [Ligand (3)]

The Schiff base ligand (**3**) (Figure 2.1c) was prepared by the condensation of 2-hydroxy-1-naphthaldehyde (1.72 g, 10 mmol), 2-hydroxy-3-methylbenzaldehyde (1.36 g, 10 mmol), with 3,4-diaminobenzoic acid (1.52 g, 10 mmol) in ethanol (75 mL, 1:1:1 molar ratio). The condensation reaction was carried out at 50 °C for 2 h. The product obtained was filtered hot, dried and preserved in a desiccator.

Yield: 79.3 %; ^{1}H-NMR (400 MHz, DMSO-d_6, δ/ ppm): 15.33(2H, s, O–H), 11.40 (H, s, O–H,acid), 9.18 (2H, s, -N=CH), 6.68-8.35 (9H, m, aromatic), ; IR (ATR, cm^{-1}): 1632 (-C=N stretching of azomethine group), 1341 (-C–O stretching of phenolic group); Anal. Calcd. for $C_{26}H_{20}N_2O_4$: C, 73.57; H, 4.75; N, 6.60. Found: C, 72.98; H, 4.43; N, 5.87.

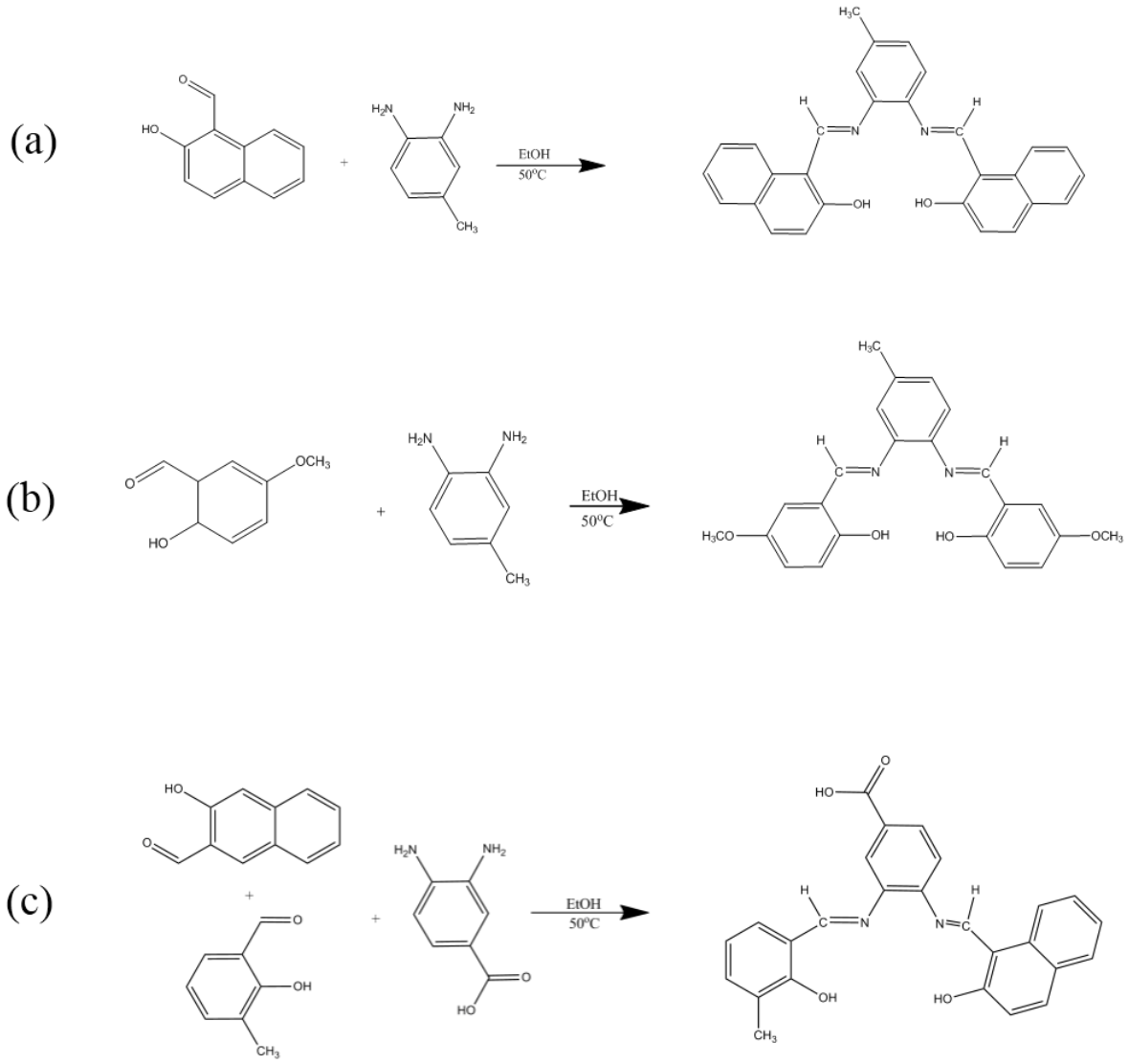

Figure 2.1: Reaction schemes for the synthesis of (a) ligand (**1**), (b) ligand (**2**) and (c) ligand (**3**).

2.2.4. Synthesis of Cobalt(II) Schiff-base complexes

2.2.4.1. Synthesis of N,N'-bis(1-naphthaldehyde)-4-methylorthophenylenediiminatocobalt [Complex (4)]

A methanolic (50 mL) solution of the cobalt(II) acetate (0.75 g, 3 mmol) was mixed drop-wise with the solution of the Schiff base (**1**) (1.18 g, 3 mmol) in methanol (90 mL). The mixture was refluxed for 3 h hours at 50 °C. On cooling, the brown solid product was collected by filtration and then washed several times with methanol. The final product was vacuum dried.

Yield: 83.7 %; IR (ATR, cm^{-1}): 1583 (-C=N stretching of azomethine group), 1360 (-C–O stretching of phenolic group) 554 (Co–O), 458 (Co–N stretching); Anal. Calcd. for $C_{29}H_{20}N_2O_2Co$: C, 71.46; H, 4.14; N, 5.75. Found: C, 70.89; H, 4.40; N, 6.05.

2.2.4.2. Synthesis of N,N'-bis(5-methoxybenzaldehyde)-4-methylorthophenylenediiminatocobalt [Complex (5)]

A methanolic (50 mL) solution of the cobalt(II) acetate (0.75 g, 3 mmol) was mixed drop-wise with the solution of the Schiff base (**2**) (1.18 g, 3 mmol) which was mixed with triethylamine (0.61 g, 6 mmol) in 90 mL methanol. The mixture was refluxed for 3 h hours at 50 °C. On cooling, the brown solid product was collected by filtration and then washed several times with methanol. The final product was vacuum dried.

Yield: 72.4 %; IR (ATR, cm^{-1}): 1588 (-C=N stretching of azomethine group), 1364 (-C–O stretching of phenolic group) 552 (Co–O), 456 (Co–N stretching); Anal. Calcd. for $C_{23}H_{20}N_2O_4Co$: C, 61.75; H, 4.51; N, 6.26. Found: C, 61.48; H, 4.70; N, 6.05.

2.2.4.3. Synthesis of N-(naphthaldehyde)- N'-(3-methylbenzylidene)benzoic cobalt(II) [Complex (6)]

A methanolic (50 mL) solution of the cobalt(II) acetate (0.44 g, 2,5 mmol) was mixed drop-wise with the solution of the Schiff base (**3**) (1.06 g, 2.5 mmol) which was mixed with triethylamine (2 ml) in methanol (90 mL). The mixture was refluxed for 3 h hours at 50 °C. On cooling, the brown solid product was collected by filtration and then washed several times with methanol. The final product was vacuum dried.

Yield: 75.6 %; IR (ATR, cm^{-1}): 1588 (-C=N stretching of azomethine group), 1359 (-C–O stretching of phenolic group) 550 (Co–O), 457 (Co–N stretching); Anal. Calcd. for $C_{26}H_{18}N_2O_4Co$: C, 64.87; H, 3.77; N, 5.82. Found: C, 64.12; H, 3.70; N, 6.19.

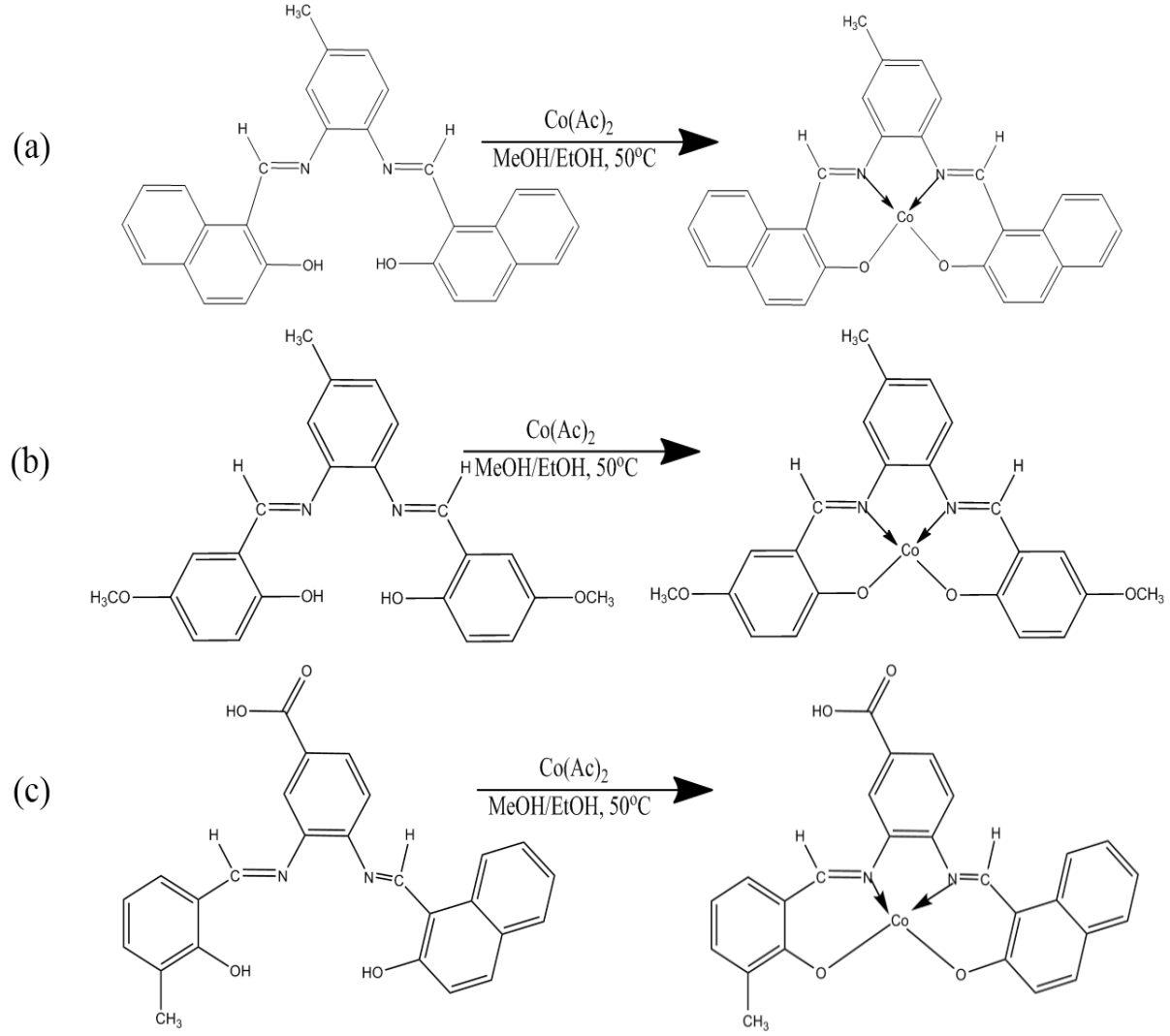

Figure 2.2: Reaction schemes for synthesis of (a) complex (**4**),(b) complex (**5**) and (c) complex (**6**).

2.3. Results and discusion

2.3.1. Characterization of the cobalt schiff base complexes

2.3.1.1. Cobalt complex (4)

Microanalyses were used to establish the purity of the Schiff bases and their metal complex. Air and moisture stable brown crystalline solid of cobalt (II) complexes were formed.

The ^{1}H NMR spectral data of the Schiff base was recorded in DMSO-d_6 against tetramethylsilane (TMS) as internal reference. The ^{1}H NMR signals due to methoxy, methyl and azomethine protons for ligand (**1**) were observed at 2.4, 9.7 and 15.2 ppm as a singlet. The aromatic protons appeared in the range of 6.98-7.39 ppm as a multiplet and the O-H protons of the phenolic groups were observed at 15.2 ppm as a singlet.

The shift observed at 1539-1560 cm^{-1} in the ligands (**1**) to 1541-1575 cm^{-1} in the complexes (**4**) (Figure 2.3) indicates the azomethine nitrogen interacting with the metal ion [23-26]. The two new bands appeared in the low frequency region of the cobalt complex at 570 cm^{-1} for $\nu_{Co—O}$ and 480 cm^{-1} for $\nu_{Co—N}$ [26, 27].

The TGA and DSC gives information about thermal stability, melting, crystallization, decomposition, sublimation, and glass transition but in this study there were used to determine the decomposition of the complex. The TGA of the cobalt(II) complex (**4**) shows a single step decomposition at 420 °C. The DSC shows an exothermic peak at 420 °C which proves the decomposition of the TGA (Figure 2.4), where the TGA showed decomposition in the region between 25 °C to 410 °C. The profile remains constant due to structural stability though the DSC in that range shows morphological transformation.

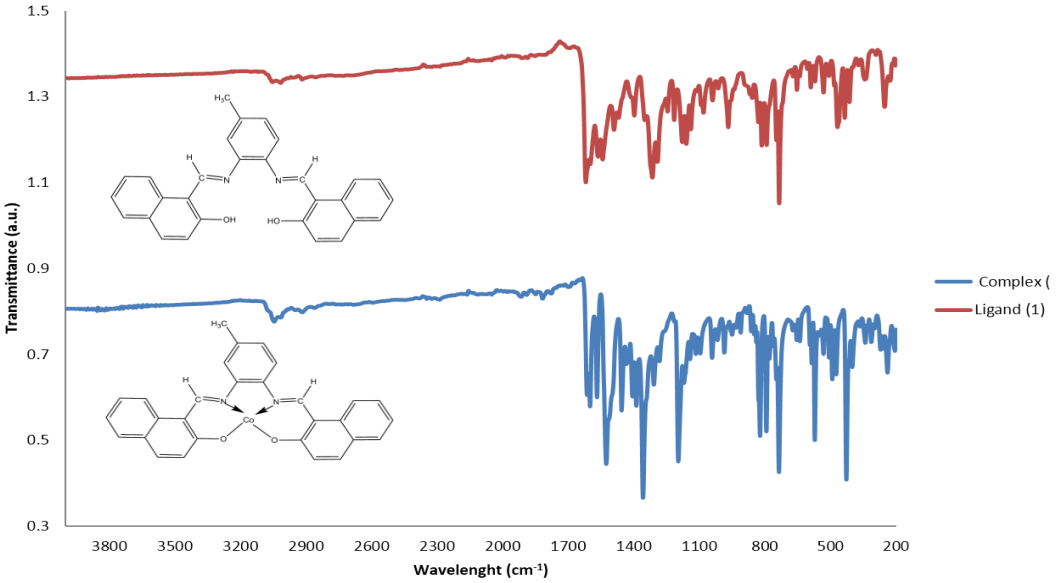

Figure 2.3: IR spectra of Schiff base ligand (**1**) and complex (**4**).

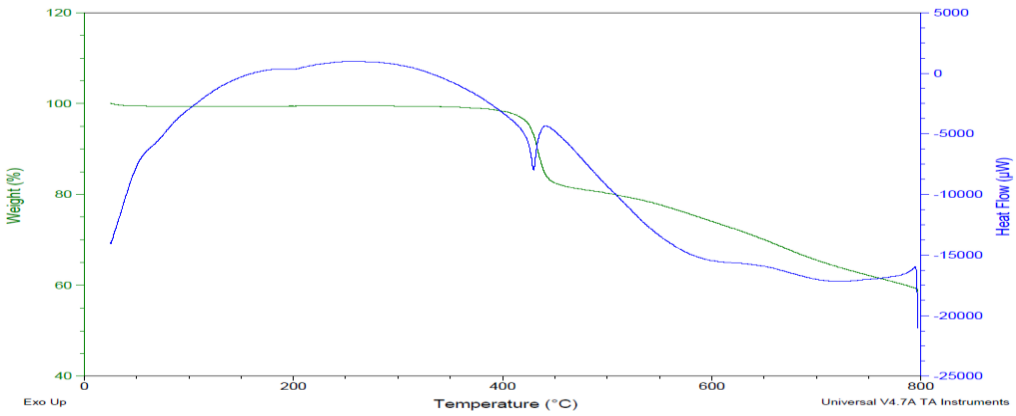

Figure 2.4: The TGA and DSC thermogram of complex (**4**).

2.3.1.2. Cobalt complex (2)

The Schiff base ligand (**2**) and its cobalt (II) complex (**2**) were isolated pure from ethanol and obtained in very good yields. The purity of the Schiff base and the metal complex as formulated were established by microanalyses. The cobalt (II) complex formed was a brown crystalline solid and stable towards air and moisture.

The ^{1}H NMR spectral data of the Schiff base was recorded in DMSO-d_6 against tetramethylsilane (TMS) as internal reference. The ^{1}H NMR signals due to methoxy, methyl and azomethine protons for N, N'-bis(5-methoxybenzaldehyde)-4-methylorthophenylenediimine ligand were observed at 3.86, 2.57 and 8.92 ppm, respectively, as a singlet. The aromatic protons appeared in the range of 6.98–7.39 ppm, as a multiplet and

the O—H protons of the phenolic groups were observed at 12.46 ppm as a singlet. The downward shift of the phenolic proton may be due to strong internal hydrogen bonding [28].

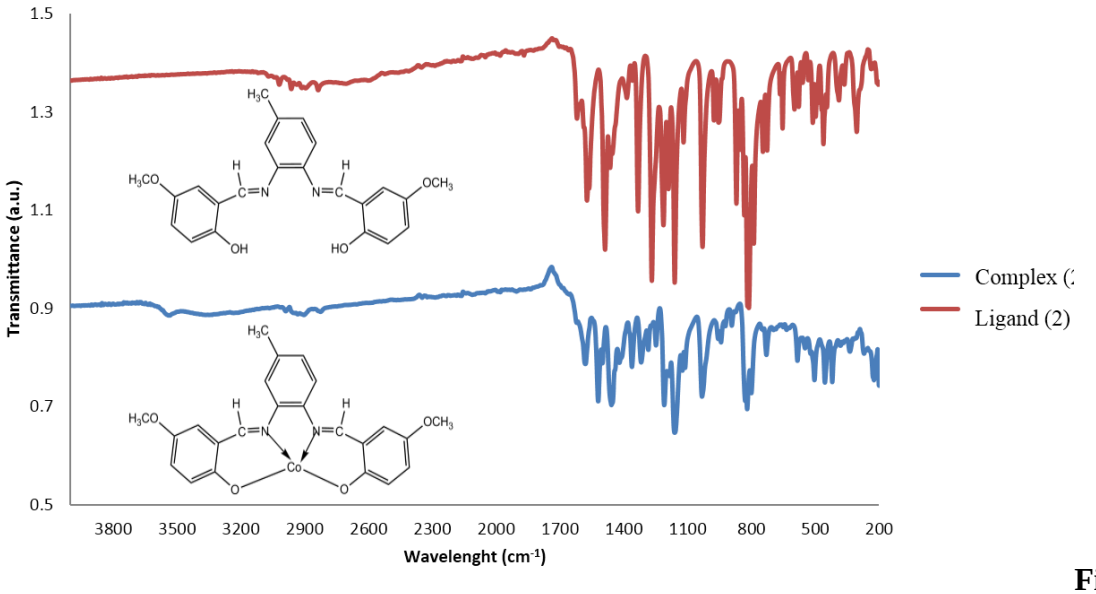

Figure 2.5: IR spectra of Schiff base ligand (**2**) and cobalt complex (**5**).

The IR spectrum (Figure 2.5) of the Schiff base ligand displayed a strong band at 1621 cm^{-1}, which is attributed to the characteristic band of the azomethine stretching frequency ($\nu_{(C=N)}$). This frequency was shifted towards the lower wave number by 33 cm^{-1} in the spectrum of cobalt complex, suggesting the coordination of nitrogen of the azomethine group to the cobalt ion in the complex [26, 27]. The $\nu_{C\text{-}O}$ stretching frequency of the Schiff base is observed at 1329 cm^{-1}, which was shifted to higher frequency region by 30 cm^{-1} in the complex indicating coordination of phenolic oxygen. The two new bands which appeared in the low frequency region of the cobalt complex at 552 cm^{-1} and 456 cm^{-1} are due to $\nu_{Co—O}$ and $\nu_{Co—N}$, respectively [26, 27]. From the above results, it could be concluded that the Schiff base is a tetradentate ligand coordinating via the azomethine *N* and the phenolic *O*.

The TGA plot (Figure 2.6) shows a three step decomposition pattern of the cobalt complex (**2**), where the first decomposition step of 7 % is a result of water loss, in the region between 100 - 110 °C. A second sharp decomposition at around 350 °C is a result of organic moiety decomposition. DSC proves the three exothermic peaks showing the decomposition at 80 °C, 350 °C and 820 °C, and at the region 140 °C to 160 °C due to morphology transformation [29].

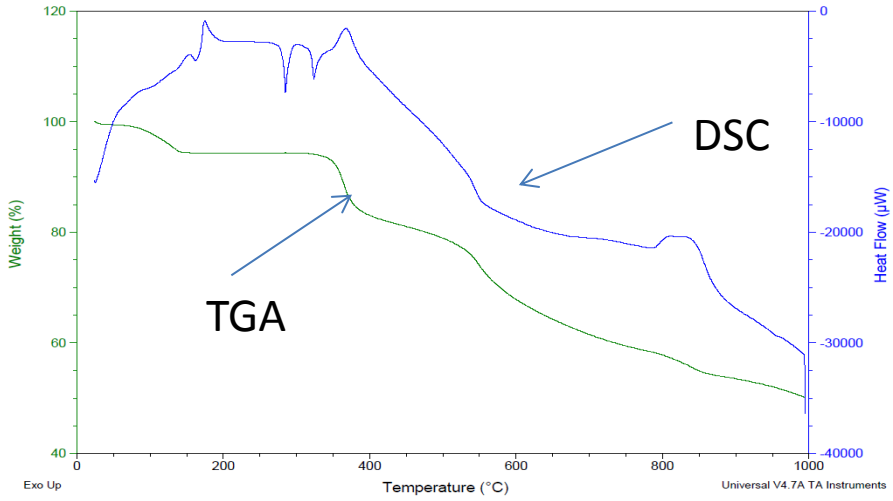

Figure 2.6: The TGA and DSC thermogram of cobalt complex (**5**).

2.3.1.3. Cobalt complex (6)

The synthetic route to prepare unsymmetrical Schiff bases were reported previous [26, 27, 30]. The ^{1}H NMR spectral of Ligand (**3**) shows the aromatic protons in the range of 6.68-8.35 ppm and the OH protons of the phenolic groups in the range of 14.4–15.3. The peak obtained at 8.2 ppm is attributable to the azomethine protons. The ^{1}H NMR peaks are similar to those reported previously [26, 30].

The IR spectrum (Figure 2.7) of the Schiff base ligand displayed a strong band at 1609–1632 cm^{-1}due to ($\nu_{(C=N)}$). of the azomethine group and the corresponding bands in the complex (**6**) were observed in the range of 1568–1632 cm^{-1} [30].

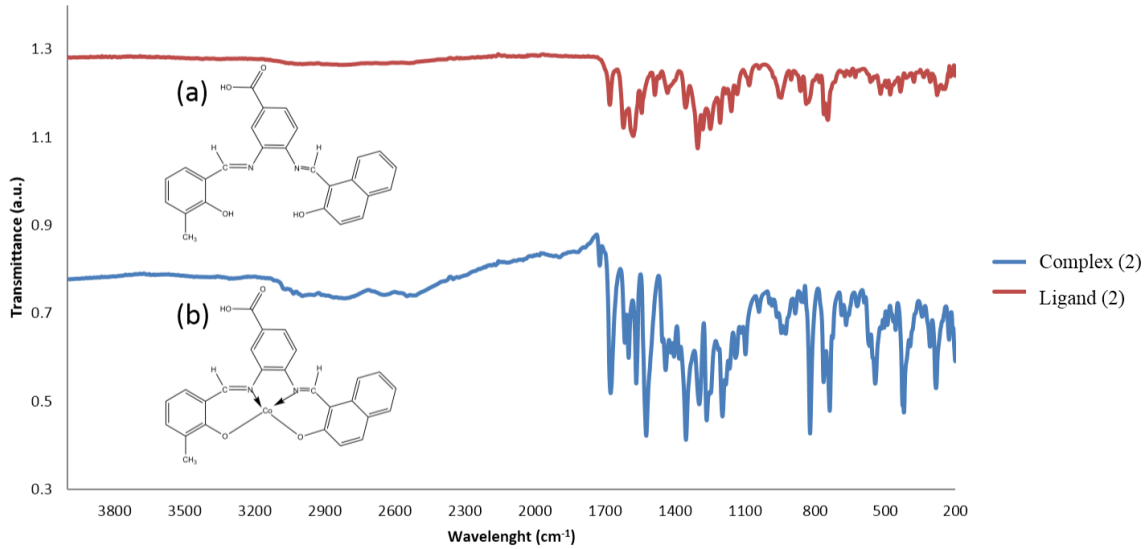

Figure 2.7: IR spectra of Schiff base ligand (**3**) and cobalt complex (**6**).

The TGA (Figure 2.8) shows a three distinct steps of decomposition. At 70 °C there is a ~5% loss of weight due to water molecule and DSC confirms the exothermic peak at that temperature. The complex was thermally stable from 70 °C up to 375 °C showing the decomposition of the organic moiety. This indicates that the complex has good stability. The DSC of the complex (**6**) exhibits an exothermic peak at 800 °C with the loss of weight in the TGA.

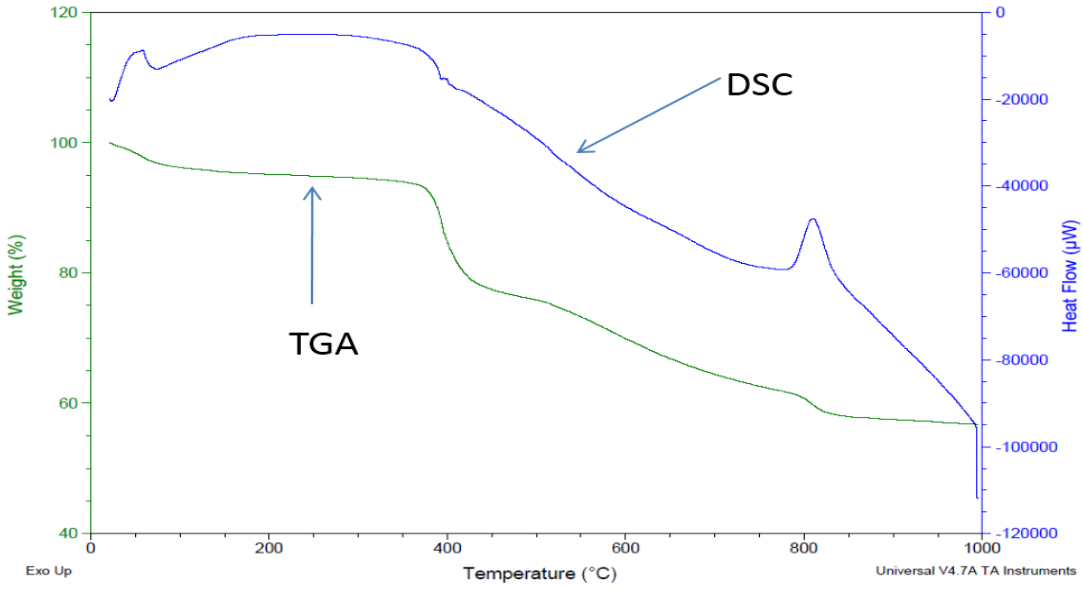

Figure 2.8: The TGA and DSC thermogram of cobalt complex (**6**).

2.4. Conclusion

A series of cobalt(II) complexes involving symmetrical tetradentate Schiff bases derived from methylorthophenylenediimine and unsymmetrical tetradentate derived from 3,4-diaminobenzoic acid have been synthesized and characterized. it was found that the Schiff base coordinated with cobalt via the azomethine nitrogen and the phenolic oxygen.

2.5. References

1. I. J. Sallomi, A. J. Shaheen; Polyhedron, 17 (1998) 1420.
2. M. H. Mahmoudkhani, A. Gorji, S. Dehghanpour, H. R. Bijanzadeh; Polyhedron, 21 (2002) 2733.
3. S. Yamada; Coord. Chem. Rev., 190 (1999) 537.
4. T. D. Thangadurai, M. Gowri, K. Natarajan; Synth. React. Inorg. Met. Org. Chem., 32 (2002) 329.
5. A. Pui; Croatica Chem. Acta, 75 (2002) 165.
6. L. Casella, M. Gullotti; Inorg. Chem., 25 (1986) 1293.
7. E. Kimura, R. Machida, M. Kochima; J. Am. Chem. Soc., 106 (1984) 5497.
8. J. W. Pyrz, A. I. Roe, L. J. Stem, J. R. Que; J. Am. Chem. Soc., 107 (1985) 614.
9. M. Turner, B. Erdogan, H. Koksal, S. Serin, M. Y. Nutku; Synth. React. Inorg. Met. Org. Chem., 28 (1998) 529.
10. W. Zishen, L. Zhiping, Y. Zhenhuan; Trans. Met. Chem., 18 (1993) 291.
11. J. Chakraborty, R. N. Patel; J. Ind. Chem. Soc., 73 (1996) 191.
12. C. P. Johnson, J. L. Atwood, J. W. Steed, C. B. Bauer, R. D. Rogers; Inorg. Chem., 35 (1996) 2602.
13. N. Alizadeh, S. Ershad, H. Naeimi, H. Sharghi, M. Shamsipur; Pol. J. Chem., 73 (1999) 915.
14. C. Ettling; Ann. Chem. Pharm., 35 (1840) 241.
15. H. Schiff; Ann. Suppl., 3 (1864) 343.
16. J. E. Huheey, E. A. Keiter, R. L. Keiter, Harper Collins College Publishers, New York 4 (1993).
17. R. H. Holm; J. Am. Chem. Soc., 82 (1960) 5632.
18. C. N. Banwell, E. M. McCash; McGraw-Hill, UK, Ch.3 (1996) 55.
19. F. W. Fifield and D. Kealey; Analytical Chemistry, Blackie, Glasgow, 2 (1990).
20. J. K. M. Sanders; Modern NMR Spec., NY: Oxford Press, 1989.
21. W.Pauli; Naturwissenschaften, 12 (1924) 741.
22. ParkinElmer products and services [Online], Available at http://www.perkinelmer.com/product/2400-chns-o-series-ii-system-100v-n2410650 (accessed 01 Feb 2016).
23. G. A. Kolawole, K. S. Patel; J. Chem.Soc., (1981) 1241.
24. K. S. Patel, G. A. Kolawole, A. Earnshaw; J. Inorg. Nucl. Chem., 43 (1981) 3107.

25. A. A. Osowole, G. A. Kolawole, O. E. Fagade; Synth. React. Inorg. Met.Org. Chem., 35 (2005) 829.

26. A. A. Nejo, G. A. Kolawole, A. O. Nejo; J. Coord. Chem., 63 (24) (2010) 4398.

27. M. M. Abd-Elza; J. Chin; Chem. Soc., 48 (2001) 153.

28. X. R. Bu, C. R. Jackson, D. V. Derveer, X. Z. You, Q. J. Meng, R. X. Wang; Polyhedron, 16 (1997) 2991.

29. C. H. Lee, C. K. Hsu, C. L. Chan; Thermochim. Acta, 173 (2002) 392.

30. A. A. Nejo , G. A. Kolawole , A. R. Opoku , J. Wolowska , P. O'Brien; Inorg. Chim. Acta, 362 (2009) 3993.

Chapter Three

Synthesis of Cobalt Nanoparticles by Thermal Decomposition of Schiff Base Complexes

Chapter Three

Synthesis of Cobalt Nanoparticles by Thermal Decomposition of Schiff Base Complexes.

3.1. Introduction

Contents

3.1. Introduction

Cobalt nanoparticles possess extraordinarily high-density magnetic properties, hardness levels, sintering reactivities and impact resistance properties. The synthesis of cobalt nanoparticles is of particular interest to researchers in the field of data storage and biomedical applications [1]. Cobalt nanoparticles exist in multiple crystal structures including the face centered cubic (fcc), hexagonally closed packed (hcp) and ε-cobalt. There is a strong correlation between crystal structure of cobalt nanoparticles and the magnetic or electronic properties. The thermal decomposition method can produce high-quality magnetic nanoparticles [2-5]. Recently methods used to prepare cobalt nanoparticles have been studied extensively including thermal decomposition [2, 3], gas vapor condensation [6, 7], reduction of cobalt salt [8, 9] and precipitation method [10]. Cobalt nanoparticles have also been synthesised by the thermal decomposition of several precursors including cobalt carbonyls, acetylacetonates, nitrosophenylhydroxylamines, acetate and Schiff bases [11-19]. For example, cobalt carbonyl ($Co_2(CO)_8$), bis(salicylidene)cobalt(II) [11] and bis(2-hydroxyacetophenato)cobalt(II) [12] were used as precursors to synthesize cobalt nanoparticles. The precursors managed to form pure cobalt cubic phase, however when the particles were exposed to air they formed cobalt oxide.

The use of single source molecular precursors in which the metal-chalcogenide bond is available has proven to be an efficient route to produce pure high-quality nanoparticles [20]. In this route, the molecular precursors are decomposed in a coordinating solvent at relatively high temperatures, hence promoting the crystallinity and passivating the nanoparticle's surfaces. A wide range of nanoparticles have been prepared using this method. The fabrication of nanoparticles from single molecule precursors is a one-step process, typically carried out at temperatures in the range 200-300 ^{o}C [21, 22].

This chapter reports the thermal decomposition of Schiff base complexes as a source of cobalt to produce cobalt nanoparticles in the presence of hexadecylamine (HDA) to prevent irreversible aggregation. Transmission electron microscopy (TEM), scanning electron microscopy (SEM), energy dispersive X-ray (EDX), X-ray diffraction (XRD) and magnetic properties are employed to characterize the properties of the cobalt nanoparticles.

3.2. Experimental

3.2.1. Materials

Hexadecylamine (HDA) and tri-*n*-octylphosphine (TOP), were purchased from Aldrich-Sigma. Ethanol, methanol and toluene were purchased from Merck. All the reagents and chemical were analytical or spectroscopic grade and used as purchased. The precursors are complexes **4** and **5**.

3.2.2. Instrumentation

The morphology, size and crystallographic properties of cobalt nanoparticles were characterized using transmission electron microscopy (TEM), scanning electron microscopy (SEM), energy dispersive X-ray (EDX) and X-ray diffraction (XRD).

3.2.2.1. Scanning Electron Microscopy (SEM)

SEM is a technique used to obtain high resolution surface information. It is largely used for characterization of nanostructures and nanomaterials. High resolution images are obtained at a very low magnification at the nanoscale range (~5-200 nm). SEM Images will appear brighter at the very high average atomic number than low average atomic number. The scattering angle depends on the atomic number in which primary electrons arriving at the given detector position, this is used to produce images containing topological and composition information [23]. In general SEM generates an electron beam that scans back and forth over a solid sample (backscattered electrons are detected). EDX and Energy

Dispersive spectroscopy (EDS) is equipped with SEM. These techniques are used to determine the morphology and the composition of the materials.

A Zeiss Ultra Plus FEG SEM was used for surface morphology analysis, equipped with an oxford detector EDX at 20 kV which uses Aztec software for elemental analysis.

3.2.2.2. Transmission Electron Microscopy (TEM)

Transmission Electron Microscopy (TEM) is typically used to obtain high resolution surface information, and it transmits a very high energy electron beam through a thin sample which is diffracted by the lattices of the crystalline materials in order to image and analyse the microstructure of the materials at the atomic scale resolution [24]. This technique involves the imaging and angular distribution analysis of the forward-scatterings electron. The images obtained by TEM can be used in structural characterisation to classify various phases of nanomaterials [25].

The morphology and particle sizes of cobalt nanoparticles were characterized by a JEOL 1400 TEM at an accelerating voltage of 120 kV. Samples were prepared by evaporating drops of diluted solution of cobalt nanoparticles. A Megaview III camera was used and the images were captured using iTEM software

3.2.2.3. Powder X-ray diffraction (p-XRD)

The patterns in which all atoms arranged themselves in the crystalline states are characterised by the periodic repetitions in 3D. XRD is used to determine the crystal structure of a solid, the lattice constants and geometry and orientation of a single crystal. It can be used to identify unknown materials [26]. Diffraction occurs when electromagnetic radiation interacts with the periodic structure whose repeat distance is about the same as the wavelength of radiation [27]. It is obtained by measuring the angles at which the X-ray beam is diffracted by the crystalline phases. The X-ray beam incident upon all atoms scatters in all directions, this can be described in terms of reflection from a set of lattice planes. The phenomenon of the X-ray beam incident is illustrated in Figure 3.1

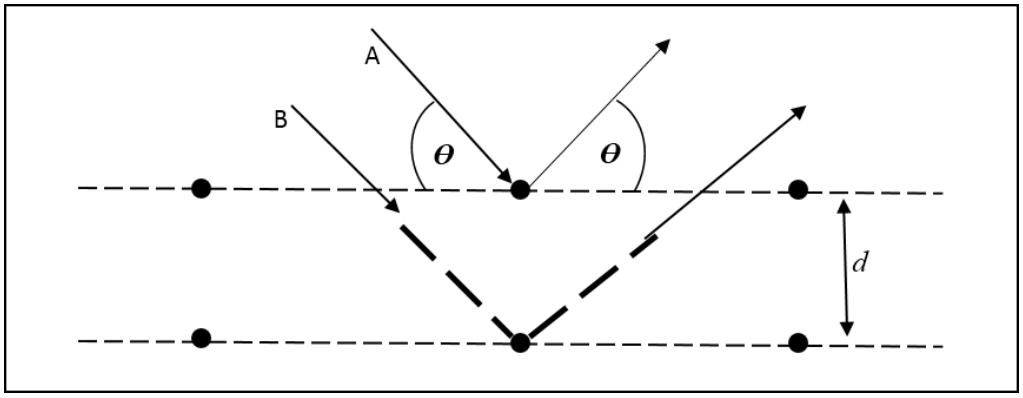

Figure 3.1: X-ray diffraction reflection geometry.

According to Bragg's Law [28], the Bragg's Equation ($n\lambda=2d \sin\theta$) relates the distance (d) between two *hkl* planes (*h*,*k* and *l* represent Miller indices of the planes) and the angle of diffractions (θ). For example the interaction of the X-rays with the sample creates the diffracted beams of X-rays which is related to the inter-planar spacing in the crystalline materials. During the analysis the wavelength λ, is known then the angle is measured. In the Equation ($n\lambda=2d \sin\theta$) n is an integer. The Debye-Scherrer equation ($D=k\lambda/\beta\cos\theta$) is used to estimate the average crystallite size of the materials at the nanoscale [29]. Identification of the crystal structure of compounds and elements can be achieved by comparing the measured intensity data of the peaks determined in the specimen with the standard data provided by the International Center for Diffraction Data (ICDD).

Powder diffraction patterns of the nanoparticles were recorded at room temperature in the angle 2θ range (20-80 °) using an advanced Bruker AXS D8 diffractometer, equipped with nickel-filtered Cu K_α radiation (λ = 1.542 Å) at 40 kV and 40 mA.

3.2.3. Synthesis of cobalt nanoparticles

3.2.3.1. Synthesis of cobalt nanoparticles by the thermal decomposition process

Cobalt nanoparticles were synthesized by the thermal decomposition of complexes (**4-5**) in hexadecylamine (HDA) which functions as both solvent and stabilizing agent [30]. In a typical procedure, the cobalt Schiff base complex (0.5 g) was dissolved in tri-n-octylphosphine (6.0 mL). The resultant solution was injected into hot HDA (6.0 g) in a three neck flask at 270 °C. The solution turned dark and a decrease in temperature was observed. The solution was allowed to stabilize at 270 °C for 2 and 4 h reaction time. Addition of excess methanol to the solution resulted in the reversible flocculation of the nanoparticles.

The flocculate was separated from the supernatant by centrifugation. The resultant cobalt nanoparticles were dissolved in toluene for characterization.

3.2.3.2. Synthesis of cobalt nanoparticles by the pyrolysis method

The cobalt nanoparticles were also synthesized by the pyrolysis of complexes (**4**-**5**). In a typical experiment, a weighed 100 mg of the complex was taken in quartz boat which was then inserted to the center of the furnace. The furnace was then heated to 450 °C and then the temperature was held at 450 °C under nitrogen gas for 1 hr. The furnace was then allowed to cool to room temperature. After cooling the residue in the quartz boat, the powder was further characterized by XRD, TEM, SEM and EDX.

3.3. Results and discussion

3.3.1. Synthesis of cobalt nanoparticles using the thermal decomposition method.

The current synthetic procedure used for the preparation of the cobalt nanoparticles was inspired by the synthesis of high-quality and monodispersed semiconductor nanoparticles in organic solvents [31-35]. The use of organometallic precursors is a well-established route for the preparation of cobalt nanoparticles.

3.3.1.1. Synthesis of cobalt nanoparticles using complex (4)

The cobalt nanoparticles were synthesized by thermal decomposition of complex (**4**) at a reaction tempereature of 270 ^{o}C for 2 and 4 hrs using 0.5 g of the precursor in hexadecylamine (HDA). Figure 3.2 shows the TEM image of cobalt nanoparticles obtained at the reaction time of 4 h. Monodispersed rod shaped cobalt nanoparticles were obtained. The average particle sizes measured from the TEM images were 3.31±0.31 nm and 74.06 ±4.2 nm for the diameter and length, respectively. There is an increase in both diameter and length of the rods as the reaction time is increased from 2 hours to 4 hours (Figure 3.2). The morphology and size of the particles depend on the thermolysis temperature and reaction time [36]. There is no agglomeration in Figure 3.2(a) showing that the particles are well dispersed [37].

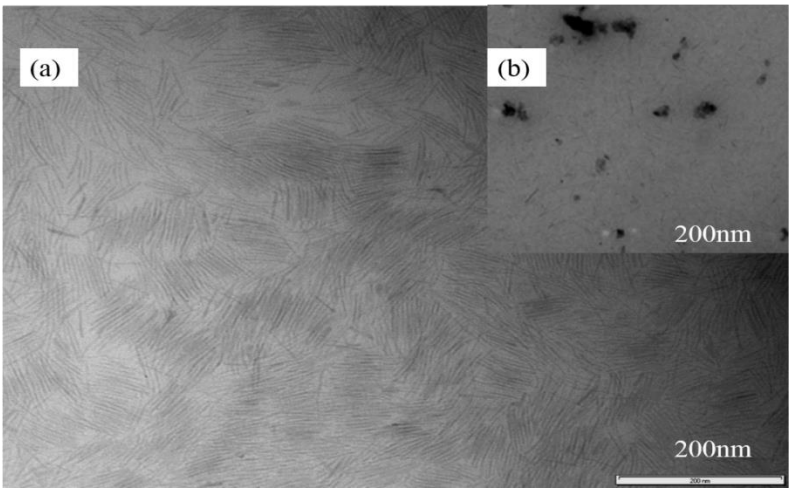

Figure 3.2: TEM image of HDA-capped cobalt nanoparticles at different reaction time, (a) 4 hrs and (b) 2 hrs.

The EDS elemental mapping (Figure 3.3a) confirms a uniform distribution of cobalt in a sample. Figure 3.3b shows EDX spectrum of cobalt nanoparticles which were prepared from complex (**1**) at 270 °C at 4 h reaction time. The EDX spectrum provides the evidence that the sample contain cobalt with a small residue as expected which is carbon and oxygen.

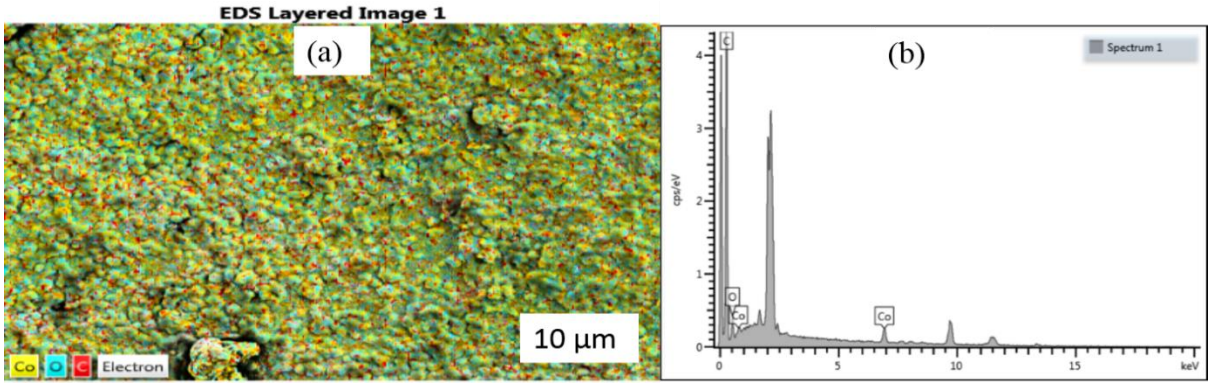

Figure 3.3: (a) EDS image and (b) EDX spectrum of HDA-capped cobalt nanoparticles prepared from complex (**4**).

The XRD pattern (Figure 3.4) of the nanoparticles synthesized from cobalt Schiff-base complex did not show any peaks of pure cobalt nanoparticles. The reflection peaks in the pattern are indexed to a mixture of cubic phases [CoO (*) and Co_3O_4 (#)] and they are consistent with the reported values of their bulk materials, CoO (ICDD #00-043-1004) and Co_3O_4 (ICDD #00-009-0418). This could be due to the oxidation of cobalt during handling and the drying process.

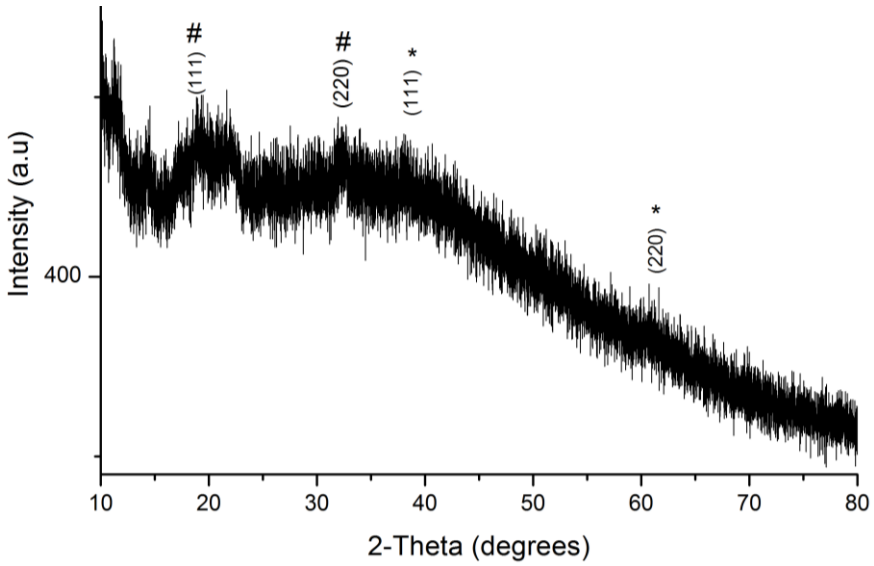

Figure 3.4: Powder XRD pattern of the HDA-capped cobalt nanoparticles prepared from complex (**4**).

3.3.1.2. Synthesis of cobalt nanoparticles using complex (5)

Complex (**5**) was thermolysed in hexadecylamine (HDA) at 270 ^{o}C for 2 and 4 hrs. Figure 3.5 (a) shows the TEM image of cobalt nanoparticles obtained at the reaction time of 2 hrs. The cobalt nanoparticles have a rod-like shape. The primary particles seemed to be single crystals of nearly uniform size.

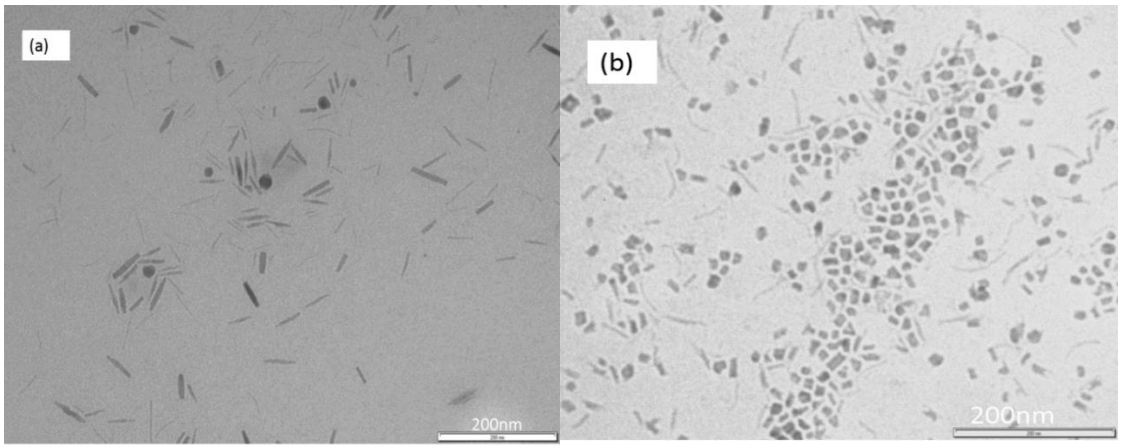

Figure 3.5: TEM images of HDA-capped cobalt nanoparticles from complex **5** at (a) 2 hrs and (b) 4 hrs reaction time.

The average particle sizes measured from the TEM images are 6.55 ± 1.44 nm (width) and 41.38 ± 8.97 nm (length). Anisotropic nanoparticles such as nanorods are usually obtained by the rapid growth in a surfactant under kinetic conditions, where the surfactant controls the

growth rate by selectively adsorbing onto a particular crystal face [2]. The growth rates on the different facets in the cobalt nanoparticles are dominated by the surface energy. The presence of the HDA as surfactant, kinetically controls the relative growth rates of different crystal planes by allowing the growth along one facet to proceed while inhibiting the growth along another facet, thereby leading to the formation of rod-like particles.

The size and morphology of nanoparticles can be controlled by varying the reaction time. As the reaction time was increased from 2 hrs to 4 hrs, the nanorods of cobalt formed were spontaneously transformed to more thermodynamically stable irregular cubic and faceted shaped nanoparticles. Figure 3.5b shows TEM images of the cobalt nanoparticles formed after 4 hrs of reaction time. It is clear from Figure 3.5b that nanoparticles exhibit a mixed morphology of irregular cubic, triangular and rod-like shaped particles with very well-defined crystalline structures. It has been established that reaction temperature above 200 ^{o}C could trigger atom diffusion which may lead to change in crystal structure or phase transition [2, 38].

To gain further insight into the features of the cobalt nanoparticles, analysis of the HDA capped cobalt nanoparticles was performed using SEM and EDX techniques. Figure 3.6a shows the SEM image of cobalt nanoparticles obtained at reaction temperature of 270 ^{o}C for 4 hrs reaction time. It is clearly seen from the SEM image that the cobalt nanoparticles are well distributed on the supports with spindle morphology. The SEM image supports the microcrystalline nature of the particles without agglomeration of the nanoparticles. The elemental analysis of the cobalt nanoparticles was performed using EDX to confirm the elements and their percentage composition. Figure 3.6b shows the EDX pattern of the cobalt nanoparticles obtained at 270 °C for reaction time of 4 hrs. The peaks of cobalt, carbon and oxygen were observed, which confirm the presence of cobalt nanoparticles. EDX measurement reveals 58.55 %, 38.16 % and 3.29 % for cobalt, carbon and oxygen respectively. There were no traces of any other impurity element observed.

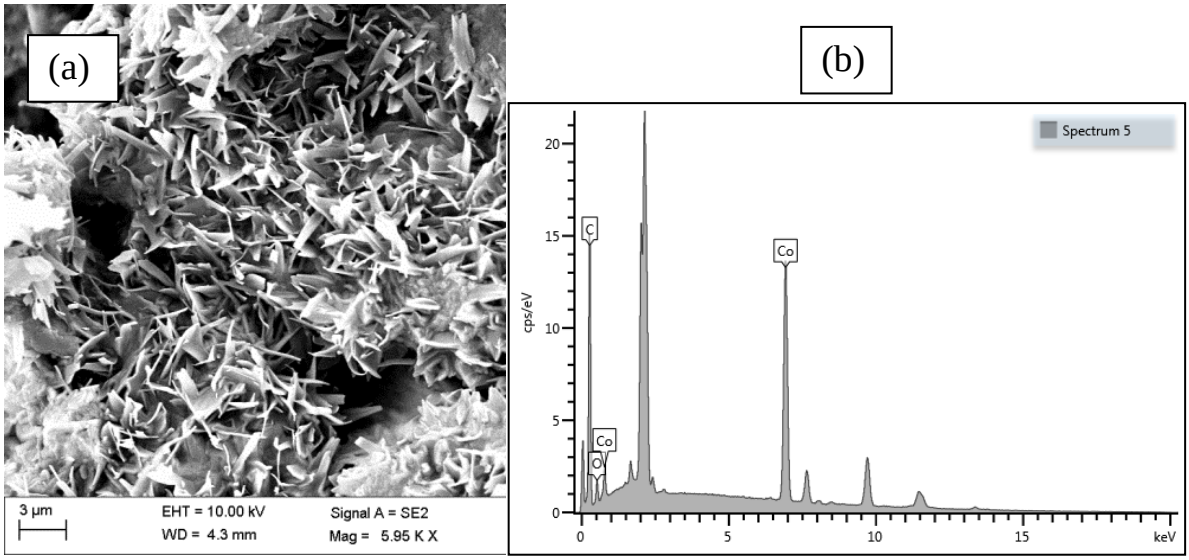

Figure 3.6: SEM image (a) and EDX pattern (b) of the HDA-cobalt nanoparticles prepared from complex (**5**) at 270 °C at 4 hrs reaction time.

The XRD pattern in Figure 3.7 shows the formation of mixture of phases: the cubic phase (#) and hexagonal phase (*) cobalt were observed [11, 39]. The (200) plane is indexed to a cubic (Co) which is consistent with the reported value of a bulk cobalt (ICDD #01-088-2325). The (100) plane is indexed to hexagonal cobalt which was identified by the reported value of cobalt bulk (ICDD #00-005-0727).

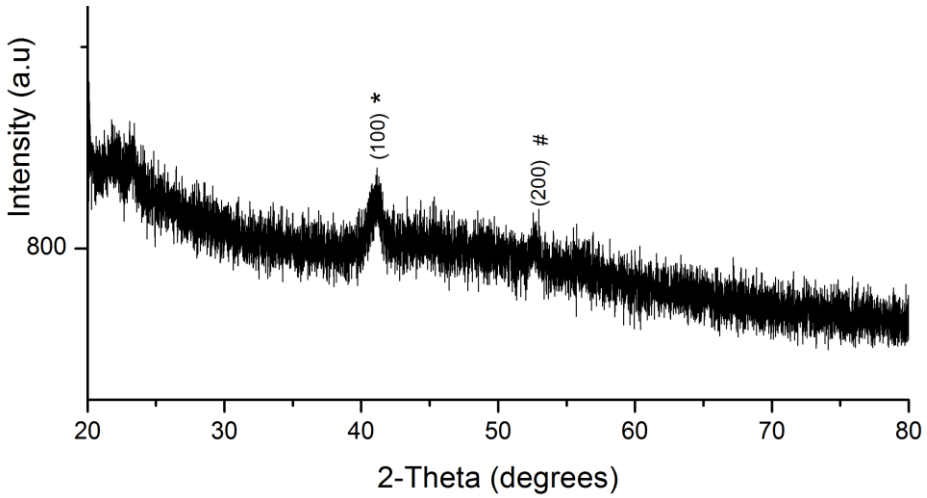

Figure 3.7: Powder XRD pattern of the HDA-capped cobalt nanoparticles synthesized from complex (**5**) at 270 °C at 4 hrs reaction time.

3.3.2. Cobalt nanoparticles synthesized by the pyrolysis method

Pyrolysis is one of the thermolysis process that is commonly used to decompose organic materials at high temperatures. Pyrolysis of a single molecule precursor using a furnace has been reported extensively [40-42]. The synthesis of cobalt nanoparticles by the pyrolysis of Schiff base complexes as a single source precursor in a furnace is described.

3.3.2.1. Cobalt nanoparticles prepared by complex (4)

The Schiff base complex shows a potential in self-capping to produce nanoparticles. Figure 3.8 shows TEM images of cobalt nanoparticles prepared by pyrolysis of complex (**4**) in a furnace at 450 °C for 1 hr. The morphology of the cobalt nanoparticles are cubic with the average particle size of 30.17 ± 5.04 nm. Figure 3.8b shows the largest particle with fine dimension of the cube. Figure 3.9 shows EDX pattern of cobalt nanoparticles with the atomic percentage of 59.5 % (O) and 40.5 % (Co). It shows high percentage of oxygen, but since the reaction was kept under inert gas that means the oxygen is from the Schiff base complex. Cobalt oxide did not form and this is supported by XRD pattern in Figure 3.10.

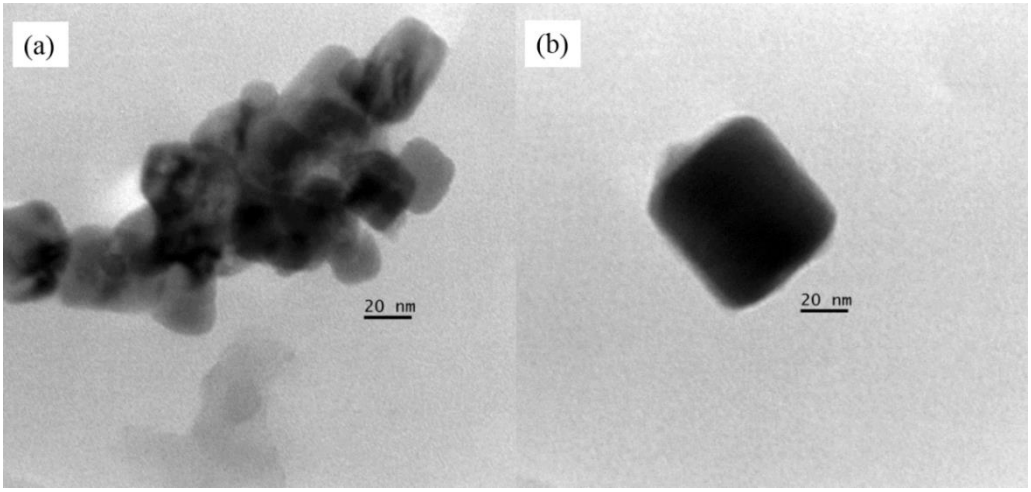

Figure 3.8: TEM image of cobalt nanoparticles prepared by pyrolysis of complex (**4**) at 450 °C for 1 hr.

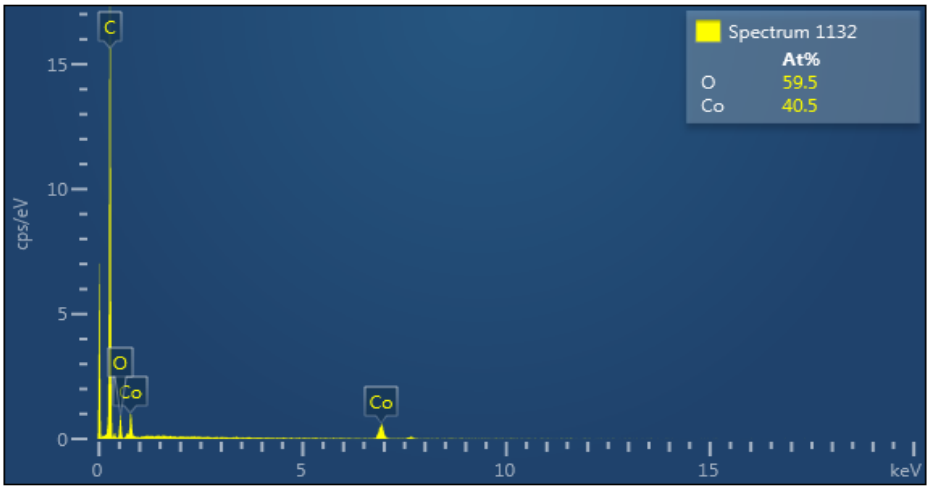

Figure 3.9: EDX pattern of cobalt nanoparticles prepared by pyrolysis of complex (**4**) at 450 °C at 1 hr.

Figure 3.10 shows the XRD pattern of pure cobalt nanoparticles prepared by pyrolysis of complex (**4**) at 450 °C for 1h. The reflection peaks are indexed as cubic Co which are consistent with those reported values of bulk Co (PDF Card: 00-015-0608). Three distinct diffraction peaks at 2θ values of 44.2°, 51.5° and 75.9° are observed corresponding to (111), (200) and (200) planes respectively.

The magnetic properties of nanomaterials with different microstructure and shape can offer a great understanding into the basics of nanomagnetism. The magnetization field depends on different shapes and microstructures of the materials [43]. Figure 3.11 is the hysteresis loop of cobalt nanoparticles prepared by the pyrolysis at 450 °C. The hysteresis loops measured at room temperature shows a ferromagnetic behaviour of the cobalt nanoparticles with the measured coercive field (H_c) of 283.93 Oe. The pyrolysis temperature does not affect the coercive field and the saturation magnetization of cobalt nanoparticles, whereas the reduction temperature has a major influence on the magnetic properties of cobalt nanoparticles [44].

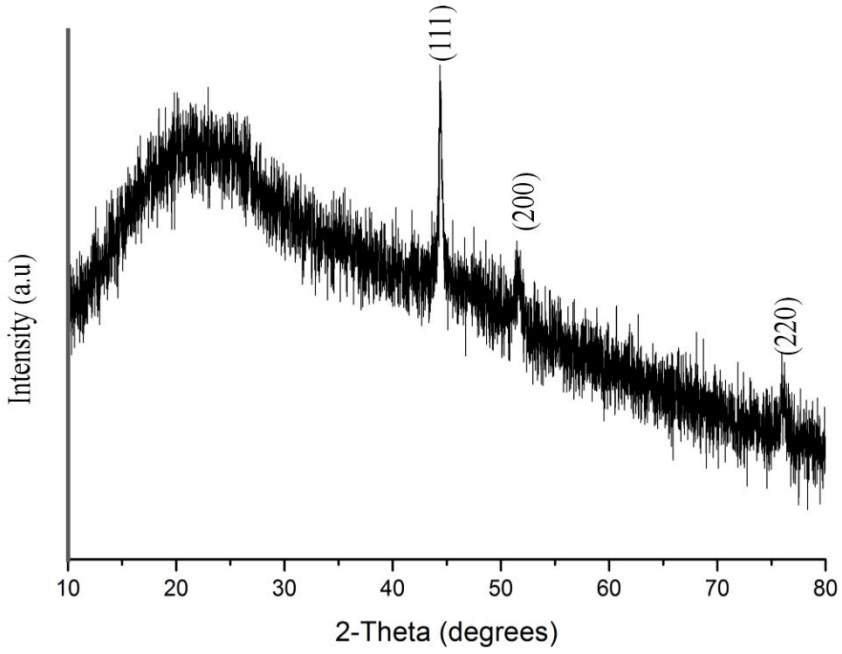

Figure 3.10: XRD pattern of cobalt nanoparticles prepared by pyrolysis of complex (**4**) at 450 °C at 1 hr.

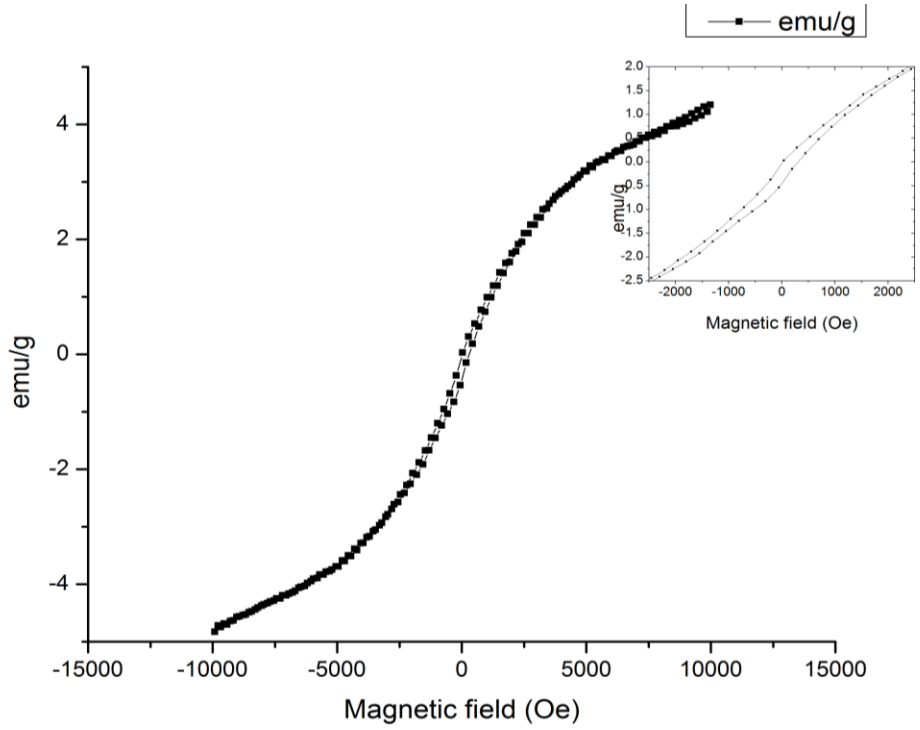

Figure 3.11: Hysteresis loop of cobalt magnetic nanoparticles prepared by pyrolysis of complex (**4**).

3.3.2.2. Cobalt nanoparticles prepared from complex (5)

The synthesis of cobalt nanoparticles by the pyrolysis method in a furnace shows a high yield nanoparticles with less impurities. Figure 3.12 is the TEM image of as-prepared cobalt nanoparticles from complex (**5**), showing cubic shaped cobalt nanoparticles with the average particle size of 14.11 nm. EDX pattern in Figure 3.13 shows a high percentage of cobalt (60.7 %) with less impurity of oxygen (39.3 %), but the XRD pattern in Figure 3.14 shows no trace of cobalt oxide.

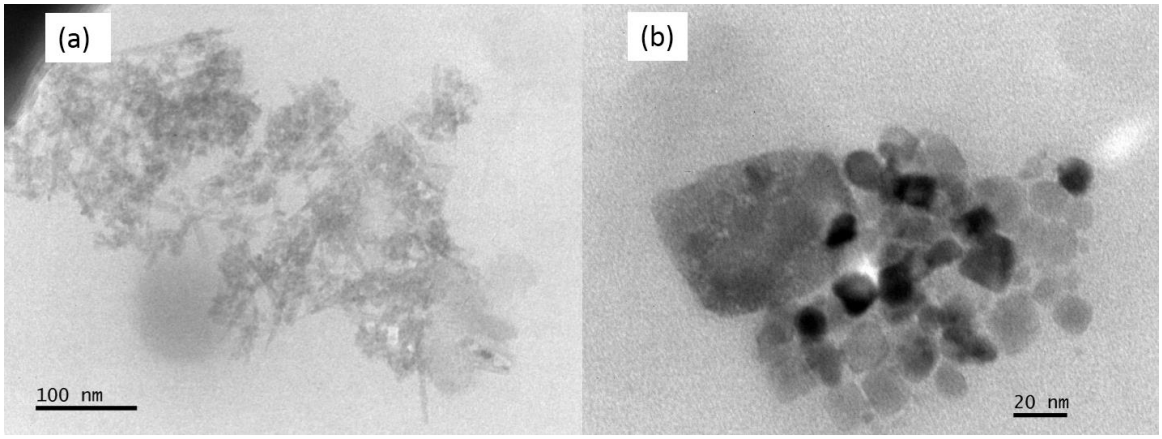

Figure 3.12: TEM image of cobalt nanoparticles prepared by pyrolysis of complex (**5**) at 450 °C at 1 hr.

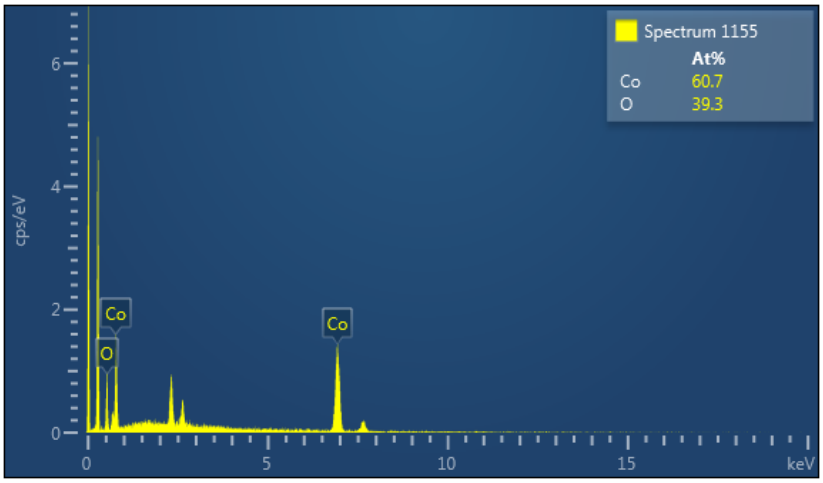

Figure 3.13: EDX pattern of cobalt nanoparticles prepared by pyrolysis of complex (**5**) at 450 °C for 1 hr.

Figure 3.14 shows the XRD pattern of cobalt nanoparticles prepared by pyrolysis of complex (**5**) at 450 °C for 1h. The main reflection peaks are indexed as cubic Co which are consistent with those reported values of bulk Co (ICDD # 00-015-0608). One distinct diffraction peak at 2θ value of 44.2° is observed corresponding to the (111) plane, the other peaks are found at 51.5° and 75.9° correspond to (200) and (200) planes respectively. Figure 3.15 is the hysteresis loop of cobalt nanoparticles prepared by the pyrolysis of complex (**5**) at 450 °C. The cycling of the magnetic field at room temperature shows a nearly linear response of magnetisation with the opening of the loop showing a coercive field, but no evidence for saturation of magnetisation. The hysteresis loops shows a ferromagnetic behaviour of the cobalt nanoparticles with the measured coercive field (H_c) of 268.47 Oe.

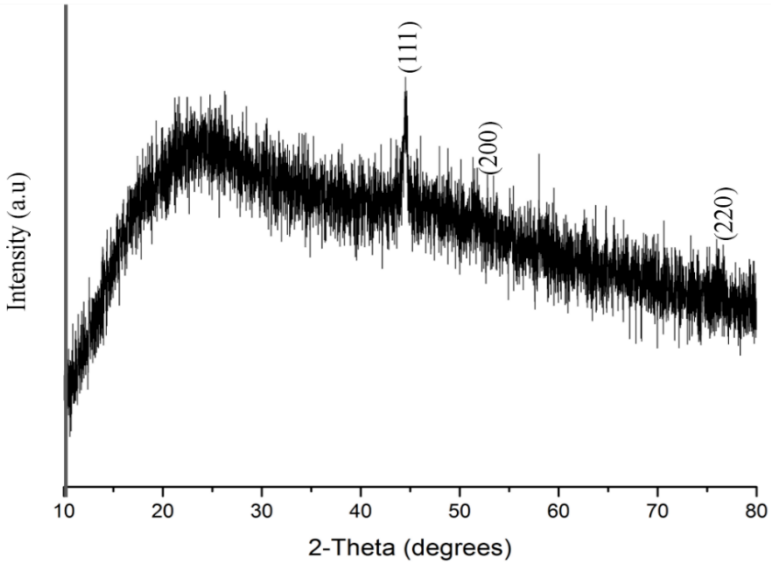

Figure 3.14: XRD pattern of cobalt nanoparticles prepared by pyrolysis of complex (**5**) at 450 °C at 1 hr.

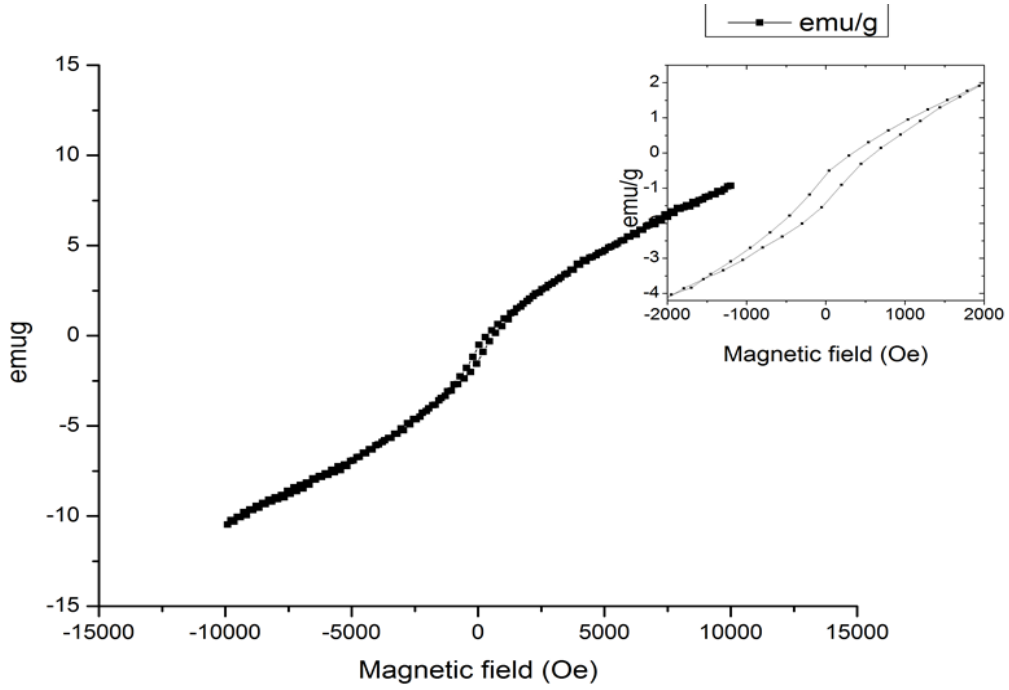

Figure 3.15: Hysteresis loop of cobalt magnetic nanoparticles prepared by pyrolysis of complex (**5**).

3.4. Conclusion

The Schiff base complexes were used to form cobalt nanoparticles by the pyrolysis and HDA capping protocols. The HDA-capped cobalt nanoparticles were formed by varying the reaction time and temperature. An increase in reaction time showed an increase in the number of particles whilst an increase in temperature showed minimization of agglomeration. Also rod and cubic shaped nanoparticles were formed the capping and pyrolysis method, respectively. Furthermore springily and smooth nanoparticles were preoduced by the capping and pyrolysis method, respectively. Chemical composition of cobalt nanoparticles prepared by both processes showed the presence of oxygen. The XRD patterns showed pure cobalt nanoparticles from those particles prepared by pyrolysis while HDA-capped cobalt nanoparticles have trace of cobalt oxide nanoparticle. These cobalt nanoparticles showed ferromagnetic behaviour. The synthesis of cobalt nanoparticles by using complex (**6**) was never been a success, it gave poor results.

3.5. References

1. J. Connolly, T. G. St. Pierre, M. Rutnakornpituk, J. S. Riffle; J. Phys., D, Appl. Phys., 37 (2004) 2475.
2. F. V. Puntes, M. K. Krishnann, P. A. Alivisatos; Science, 291 (2001) 2115.
3. C. B. Murray, S. Sun, W. Gaschler; IBMJ. Res. Dev. 45 (2001) 47.
4. M. Green; Chem. Commun. (2005) 3002.
5. T. Mthethwa, V. S. R. Pullabhotla, P. S. Mdluli, J. W. Smith, N. Revaprasadu; Polyhedron, 28 (2009) 2977.
6. X. L. Dong, C. J. Choi, B. K. Kim; Scripta Mater., 47 (2002) 857.
7. Z. H. Wang, C. J. Choi, B. K. Kim, Z. D. Zhang; J. Alloys Compd., 351 (2003) 319.
8. S. Sun, C. B. Murray; J. Appl. Phys., 85 (1999) 4325.
9. C. Luna, M. P. Morales, C. J. Serna, M. Vazquez; Mater. Sci. Eng. C, 23 (2003) 1129.
10. Y. Ichiyanagi, S. Yamada; Polyhedron, 24 (2005) 2813.
11. M. Salavati-Niasari, F. Davar, M. Mazaheri, M. Shaterian; J. Magn. Magn. Mater., 320 (2008) 575.
12. M. Salavati-Niasari, Z. Fereshteh, F. Davar; Polyhedron, 28 (2009) 1065.
13. J. Park, K. An, Y. Hwang, J. G. Park, H. J. Noh, J. Y. Kim, J. H. Park, N. M. Hwang, T. Hyeon; Nat. Mater., 3 (2004) 891.
14. S. Sun, H. Zeng, D. B. Robinson, S. Raoux, P. M. Rice, S.X. Wang, G. Li; J. Am. Chem. Soc., 126 (2004) 273.
15. F. X. Redl, C. T. Black, G. C. Papaefthymiou, R. L. Sandstrom, M. Yin, H. Zeng, C.B. Murray, S. P. O'Brien; J. Am. Chem. Soc., 126 (2004) 14583.
16. J. Rockenberger, E. C. Scher, A. P. Alivisatos; J. Am. Chem. Soc., 121 (1999) 11595.
17. D. Farrell, S. A. Majetich, J. P. Wilcoxon; J. Phys. Chem. B, 107 (2003) 11022.
18. N. R. Jana, Y. Chen, X. Peng; Chem. Mater., 16 (2004) 3931.
19. A. C. S. Samia, K. Hyzer, J. A. Schlueter, C. J. Qin, J. S. Jiang, S. D. Bader, X. M. Lin; J. Am. Chem. Soc., 127 (2005) 4126.
20. N. Revaprasadu and S. N. Mlondo; Pure Appl. Chem., 78 (2006) 1691.
21. C. B. Murray, K. R. Kagan, M. G. Bawendi; Ann. Rev. Mater. Sci., 30 (2000) 545.
22. C. B. Murray, D. J. Norris, M. G. Bawendi; J. Am. Chem. Soc., 115 (1993) 8706.
23. D. E. Newbury, D. C. Joy, P. Echlin, C. E. Fiori, J. I. Goldstien; Plenum Press, New York (1987).

24. The Hebrew University of Jerusalem, TEM Basics, [Online], Available at http://www.nanoscience.huji.ac.il/unit/tem basics.htm, (accessed 01 Feb 2016).

25. Z. L. Wang; Wiley-VCH, Weinheim Ch. 2 (2000).

26. Z. L. Wang; Wiley-VCH, Weinheim Ch.3 (2000) 37-80.

27. University of Wisconsin-Madison, Materials Research Science and Engineering Center for Nanostructured Interfaces, X-Ray Diffraction and Scanning Probe Microscopy, [Online], Available at http://mrsec.wisc.edu/Edetc/modules/xray/Xraystm.pdf, (accessed 01 Feb 2016).

28. Powder Diffraction-Inorganic Compounds, JCPDS International Conference for Diffraction Data, Philadelphia, (1984).

29. J. W. Jeffrey; Methods in X-Ray crystallography, London: Academic Press, (1971).

30. L. D. Nyamen, V. S. Rajasekhar Pullabhotla, A. A. Nejo, P. Ndifon, N. Revaprasadu; New J. Chem., 35 (2011) 1133.

31. L. D. Nyamen, V. S. R. Pullabhotla, A. A. Nejo, P. Ndifon, J. Warner, N. Revaprasadu; Dalton Trans., 41 (2012) 8297.

32. L. D. Nyamen, V. S. R. Pullabhotla, A. A. Nejo, P. Ndifon, N. Revaprasadu; New J. Chem., 35 (2011) 1133.

33. N. Pradhan, B. Katz, S .Efrima; J. Phys. Chem., 107 (2003) 13843.

34. T. Mandal, V. Stavila, I. Rusakova, S. Ghosh, K. H. Whitmire; Chem. Mater., 21 (2009) 5617.

35. J. C. Bruce, N. Revaprasadu, K. R. Koch; New J. Chem., 31 (2007) 1647.

36. E. So´wka; Physica B, 384 (2006) 282.

37. H. Shao; J. Magn. Magn. Mater. 304 (2006) 41.

38. M. H. Yang, C. P. Flynn; Phys. Rev. Lett., 62 (1989) 1476.

39. D. J. Sellmyer, M. Zheng, R. Shomski; J. Phys. Condensed Matter., 13 (2001) R433.

40. S. Ghoshal, L. B. Kumbhare, V. K. Jain, G. K. Dey; Bull. Mater. Sci., 30 (2007) 173.

41. G. Kedarnath, V. K. Jain, S. Ghoshal, G. K. Dey, C. A. Ellis, R. T. Tiekink; Eur. J. Inorg. Chem., (2007) 1566.

42. A. M. Palve, S. S. Garje; Bull. Mater. Sci., 34 (4) (2011) 667.

43. S. J. Bao, C. M. Li, C. X. Guo, Y. Qiao; J. Power Sources, 180 (2008) 676.

44. N. Shatrova, A. Yudin, V. Levina, E.Dzidziguri, D. Kuznetsov, N. Perov, J. Issi; Mater. Res.h Bull., 86 (2017) 80.

Chapter Four

Cobalt Schiff Base Complexes: Single Source Precursor for Cobalt Sulfide (Co_9S_8 and Co_3S_4) Nanoparticles

Chapter Four

Cobalt Schiff Base Complexes: Single Source Precursor for Cobalt Sulfide (Co_9S_8 and Co_3S_4) Nanoparticles

4.1. INTRODUCTION

Contents

4.1. Introduction

Transition metal sulfides have attracted a great attention recently because of their rich structural diversities and unique electronic and magnetic properties [1]. Cobalt sulfide is an important material because of the Co-S bond and its use as a hydro-sulfurization catalyst in magnetic devices [2, 3]. The bonds between cobalt and sulfur exist in various forces with few forms of binding mechanism, such as ionic bond, covalent bond and metallic bond in a molecule [4]. Cobalt sulfide is a complicated transition metal sulfide with a large number of phases and chemical composition [5]. It exists in a large number of phases as Co_xS_y, such as CoS, CoS_2, Co_2S_3, Co_3S_4, Co_4S_3 and Co_9S_8 [6, 7]. Therefore the fabrication of cobalt sulfide is a challenge as a small variation of the synthetic parameters complicates the phase diagram of Co-S systems. Shape control of cobalt sulfide is also a challenging issue because of the stoichiometry caused by co-existence of strongly reducible cobalt ion and oxidizable sulfide ion [8]. Recently, Co-S nanoparticles have been used in various applications such as solar energy absorbers [9] and ultra-density magnetic recording [10]. Co_9S_8 have been used as counter electrodes in dye sensitized solar cells in which it collects electrons from an external circuit and speeds up the reduction of I^{3-} for dye degradation [11-15]. It is also used in Li-ion batteries [16-18].

Single source precursors have recently become a preferred approach towards the synthesis of metal chalcogenide thin films and nanoparticles by colloidal and chemical vapour deposition methods [19-24]. Different methods have been applied in the synthesis of cobalt sulfide nanoparticles. O'Brien and co-workers used di-t-butyldithiophosphinatocobalt(II) as a single source precursor to synthesize cubic cobalt sulfide nanoparticles (Co_9S_8) by thermolysis in presence of tri-n-octylphosphine oxide and hexadecylamine as capping agents at the temperature of 300 °C [25]. The complexes, 1,1,5,5-tetraisopropyl-2-thiobiuret and 1,1,5,5-tetramethyl-2,4-dithiobiuret were used as single source precursors in hexadecylamine, octadecylamine or oleylamine at 230 °C to give cubic and hexagonal nanoparticles [26]. These cobalt sulfide nanoparticles have various morphologies including trigonal prisms, spheres and hexagonally faceted nanoparticles. The hydrothermal method was used to synthesize nanocrystals (Co_3S_4) and spheres (CoS) [27]. Other methods reported to synthesize the cobalt sulfide nanoparticles include pyrolysis, solvothermal decomposetion method [28, 29], template confined growth [30, 31]. Cobalt sulfide thin films have also been fabricated using the AACVD method to make thin films. O'Brien and co-workers used the AACVD method to deposit cobalt sulfide (CoS_2, Co_3S_4 and $Co_{1-x}S$) thin films by using cobalt complex of methyl n-hexyldithiocarbamate as a single source precursor [32]. These thin films were produced at the deposition temperature of 425 °C, 450 °C and 475 °C and obtained a hexagonal ($Co_{1-x}S$), pure phase (cubic Co_3S_4) and cubic (CoS_2) phase respectively.

To avoid nanoparticles from irreversible aggregation growth and to prepare a monodisperse colloid, capping agents are used. Thiols have been used as capping agent and sulfur source to synthesize cobalt sulfide nanoparticles. There are many reported sulfur sources such as L-cysteine [33], H_2S [34], Na_2S [35, 36], and thiourea [37].

This chapter reports a one-pot synthetic approach towards the preparation of cobalt sulfide nanoparticles, where new Schiff base complexes are used as sources of cobalt while 1-dodecanethiol (DDT) is utilized both as capping agent and sulfur source. The influence of ligands and reaction time on the quality of the nanoparticles is also investigated.

4.2. Experimental

4.2.1. Materials

All reagents and solvents were of analytical/spectroscopic grades and used without further purification. Tri-octylphosphine (TOP), methanol and 1-dodecanethiol were purchased from Aldrich-Sigma Company.

4.2.2. Instrumentation

The crystalline phase of the as-prepared cobalt sulfide nanoparticles was identified by XRD. The morphology and particle sizes of the synthesized nanoparticles were characterized TEM; High resolution transmission electron microscope (HR-TEM) and selected area electron diffraction (SAED). Further surface morphology of the nanoparticles were observed by SEM, equipped with EDX for elemental analysis.

All the instruments characterization techniques are explained in chapter two.

4.2.3. Synthesis of cobalt sulfide nanoparticles.

The cobalt sulfide nanoparticles were synthesized by thermal decomposition of complexes (**4-5**) in 1-dodecanethiol (DDT) using a previously reported method [38]. DDT is well known as a soft base, and by theory of hard-soft acid-base, a soft base binds strongly with a soft acid than that of a soft base with a hard acid, Co^{+2} is a soft acid. DDT has been used in a one-pot synthesis as a sulfur source and the stabilizing agent for the synthesis of Cu_2S-$CuInS_2$ nanomaterials [39]. In a typical procedure, a cobalt Schiff base complex (0.5 g) was dissolved in tri-n-octylphosphine (6.0 mL). The resultant solution was then injected into hot DDT (6.0 g) in a three necked flask at 270 °C. The solution turned dark and a decrease in temperature was observed. The solution was allowed to stabilize at 270 °C for 4 and 8 hrs reaction time. Addition of excess methanol to the solution resulted in the reversible flocculation of the nanoparticles. The flocculate was separated from the supernatant by centrifugation. The resultant cobalt nanoparticles were dissolved in toluene for characterization.

4.3. Results and discussion

4.3.1. Cobalt sulfide nanoparticles synthesized from complex (4)

The detailed structural information of the nanoparticles was further carried out using TEM, SEM, HR-TEM and SAED techniques. Figure 4.1 shows the TEM images of cobalt sulfide nanoparticles capped by 1-dodecanethiol synthesized at 270 °C for 4 hrs. The cobalt sulfide particles appear agglomerated which makes it difficult to measure their sizes. Figure 4.2 shows the TEM images of cobalt sulfide nanoparticles which are prepared from complex 1 for 8 hrs. The images also show undefined agglomerated particles with sizes larger than those synthesized at 4 hrs. This growth process is influenced by parameter (time) in which the longer growth time results in thermodynamically stable shapes of nanoparticles [40].

The SEM images of the nanoparticles prepared from complex (**4**) are presented in Figure 4.3 (4 hrs) and Figure 4.4 (8 hrs). The surface morphology of the cobalt sulfide nanoparticles from Figure 4.3a and b show nearly spherical shaped particles. The transformation of shape from spherical to undefined shapes in Figure 4.4 is caused by the effect of time as a parameter [40]. Figure 4.4 shows large particles agglomerated forming platelets resulting in a smoother surface.

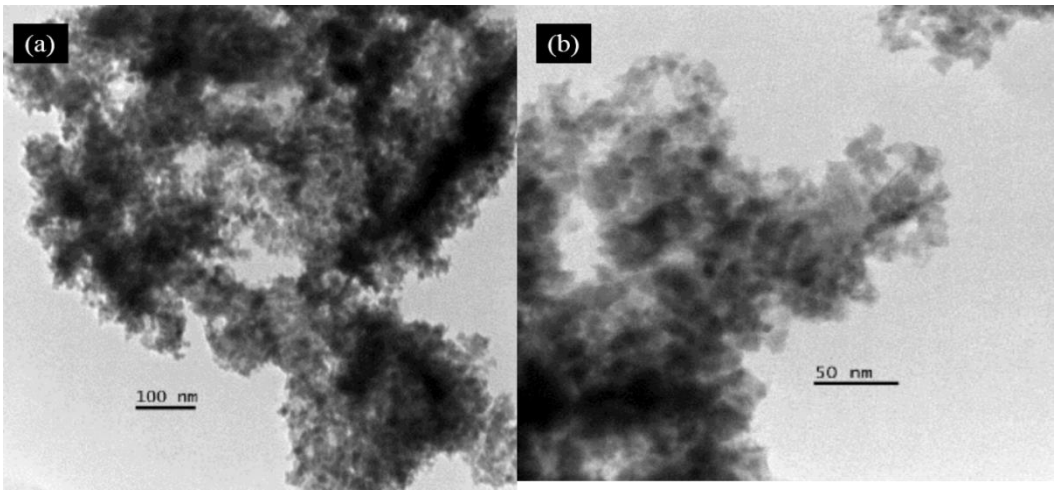

Figure 4.1: TEM images of 1-dodecanethiol-capped cobalt sulfide nanoparticles thermolysed from complex (**4**) at 270 °C for 4 hrs.

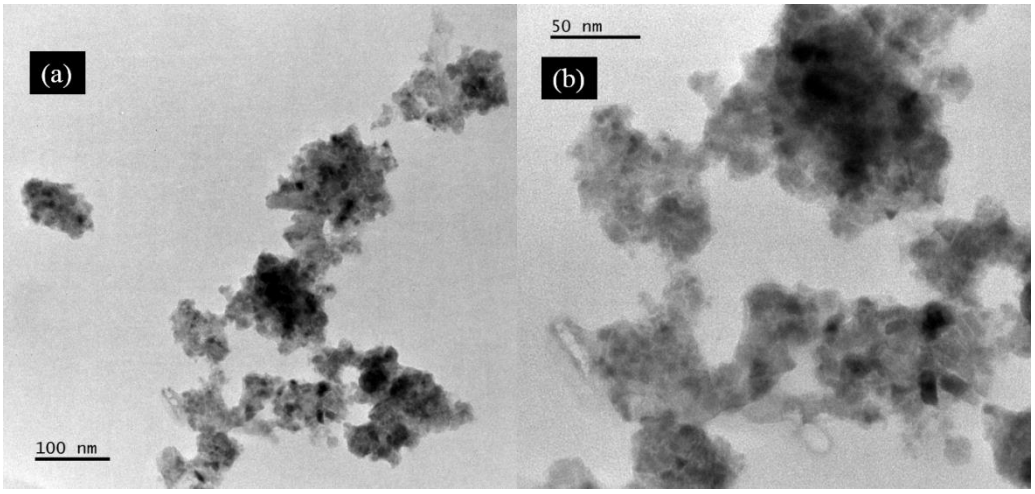

Figure 4.2: TEM images of 1-dodecanethiol-capped cobalt sulfide nanoparticles thermolysed from complex (**4**) at 270 °C for 8 hrs.

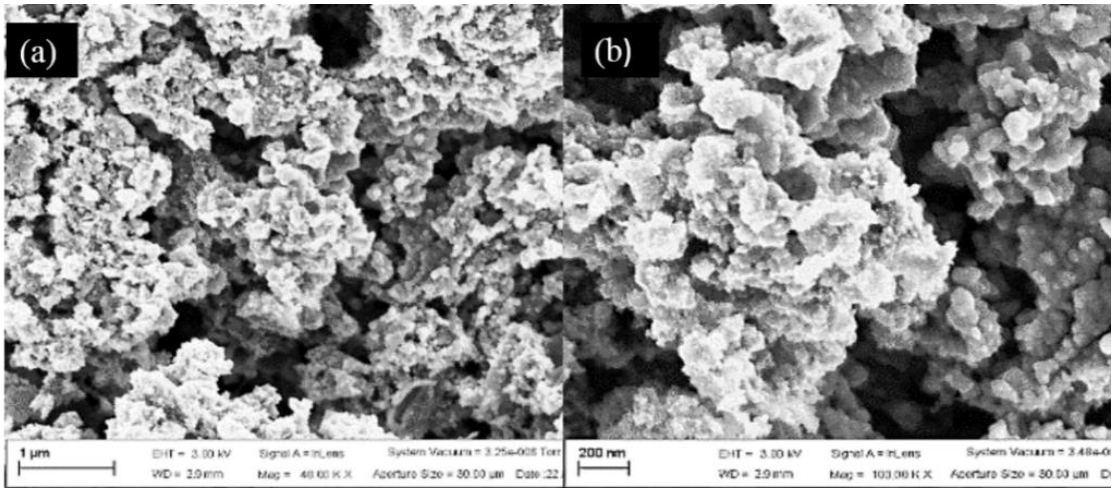

Figure 4.3: SEM images (a, b) of complex (**4**) thermolysed at 270 °C for 4 hrs.

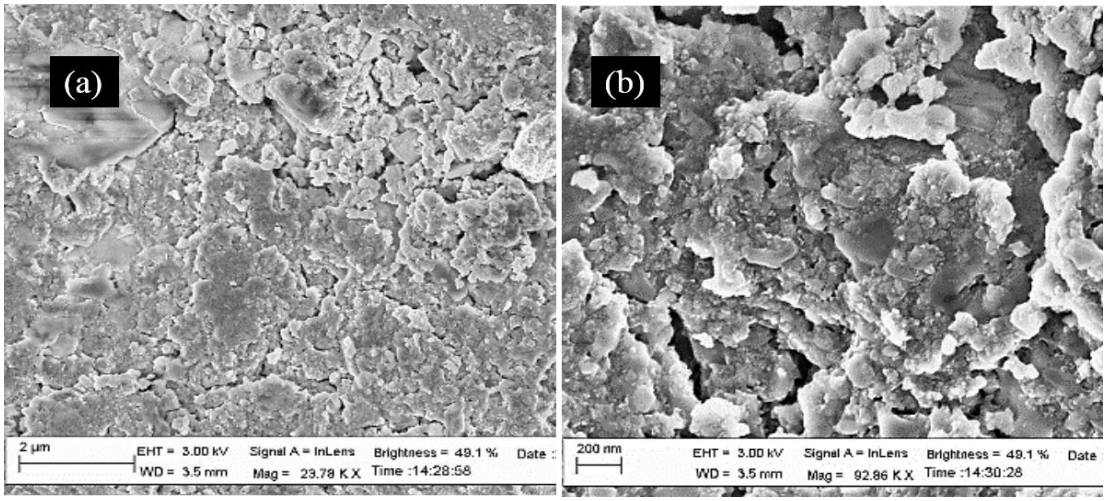

Figure 4.4: SEM images (a, b) of complex (**4**) thermolysed at 270 °C for 8 hrs.

The EDX of cobalt sulfide nanoparticles prepared from complex (**1**) synthesized at 270 °C for 4 hrs (Figure 4.5a) and 8 hrs (Figure 4.5b) shows a high atomic percentage of sulfur which indicates that sulfur from DDT bonds to cobalt during nucleation growth phase. The atomic and weight percentages are shown in Table 4.1.

Figure 4.6a shows the HR-TEM image and Figure 4.6(b) shows the SAED pattern of cobalt sulfide nanoparticles obtained from complex (**1**) at 270 °C for 4 hrs. The HR-TEM image shows well defined lattice fringes calculated to be 2.94 Å and 1.73 Å corresponding to the (311) and (440) planes of Co_9S_8 phase (ICDD #01-073-6395) respectively. The SAED pattern shows the diffraction rings which are indexed to the (311) and (440) planes of the same phase.

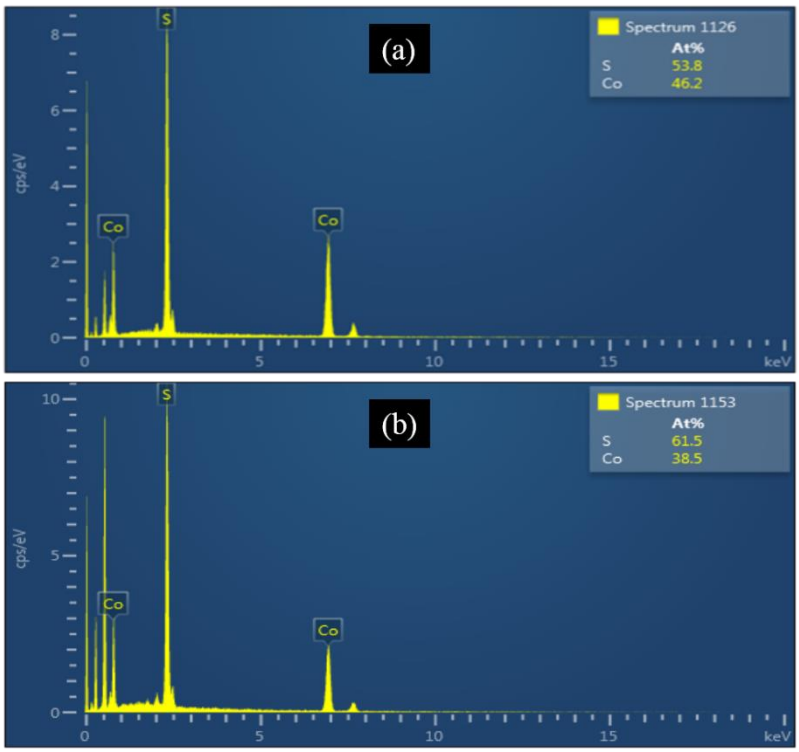

Figure 4.5: EDX patterns of complex (**1**) thermolysed at 270 °C for (a) 4 hrs and (b) 8 hrs.

Table 4.1: Weight and atomic percentage of cobalt and sulfur prepared from complex (**4**).

Time (hrs)	Weight %		Atomic %	
	Cobalt (Co)	Sulfur (S)	Cobalt (Co)	Sulfur (S)
4	61.23	38.77	46.2	53.8
8	53.53	46.47	38.5	61.5

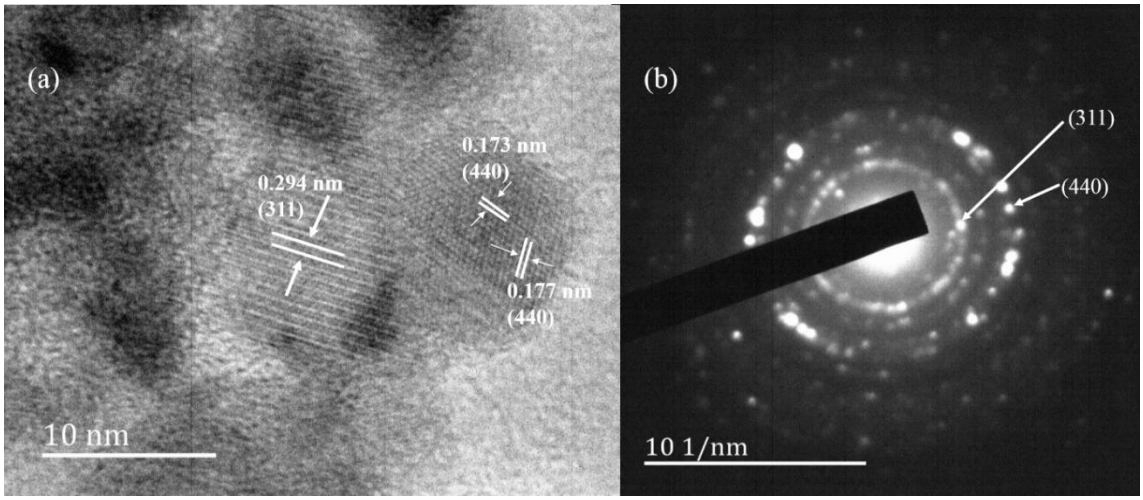

Figure 4.6: (a) HR-TEM image of cobalt sulfide nanoparticles obtained from complex (**4**) at 270 °C for 4 hrs and (b) the corresponding SAED pattern.

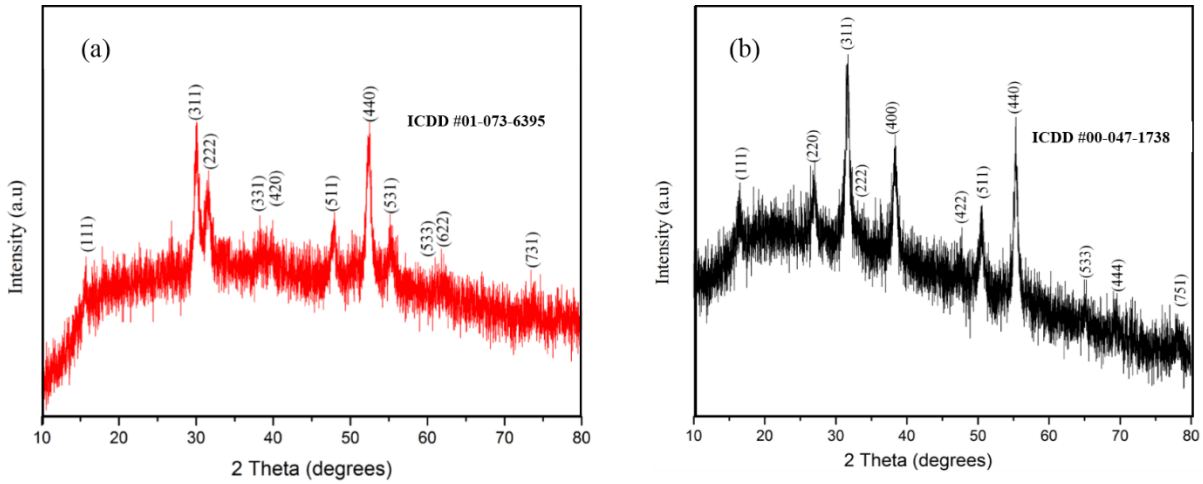

Figure 4.7: X-ray diffraction pattern of cobalt sulfide nanoparticles prepared from complex (**4**) at 270 °C at (a) 4 hrs and (b) 8 hrs reaction time.

Figure 4.7 shows the X-ray diffraction (XRD) patterns of the as-prepared cobalt sulfide nanoparticles obtained using complex (**4**) at 270 °C for (a) 4 hrs and (b) 8 hrs. The reflection peaks in Figure 4.7a can be indexed to a cubic Co_9S_8 (Cobaltpentlandite) which is consistent with the reported values of bulk Co_9S_8 (ICDD #01-073-6395). Figure 4.7b shows the XRD pattern obtained for 8 hrs of reaction at 270 °C with the reflection peaks indexed to cubic Co_3S_4 (Linnaeite) which are perfectly identified by the reported values of the bulk Co_3S_4 (ICDD #00-047-1738). Both patterns show no peaks from impurities which indicate the high purity of the product. The crystallite size (*d*) of both Co_9S_8 and Co_3S_4 nanoparticles

were estimated by the Scherrer formula (d=0.89λ/βcosθ) [41, 42] and were found to be 12.44 nm and 15.43 nm respectively.

4.3.2. Cobalt sulfide nanoparticles synthesized from complex (5)

TEM images (Figure 4.8) shows very small sized cobalt sulfide nanoparticles agglomerated. Figure 4.9 shows the SEM images of the cobalt sulfide nanoparticles at different magnification prepared by complex (**5**) at 270 °C for 4 hrs. The SEM shows a uniformly distributed spherical shape particles with the average diameter of 0.6 µm.

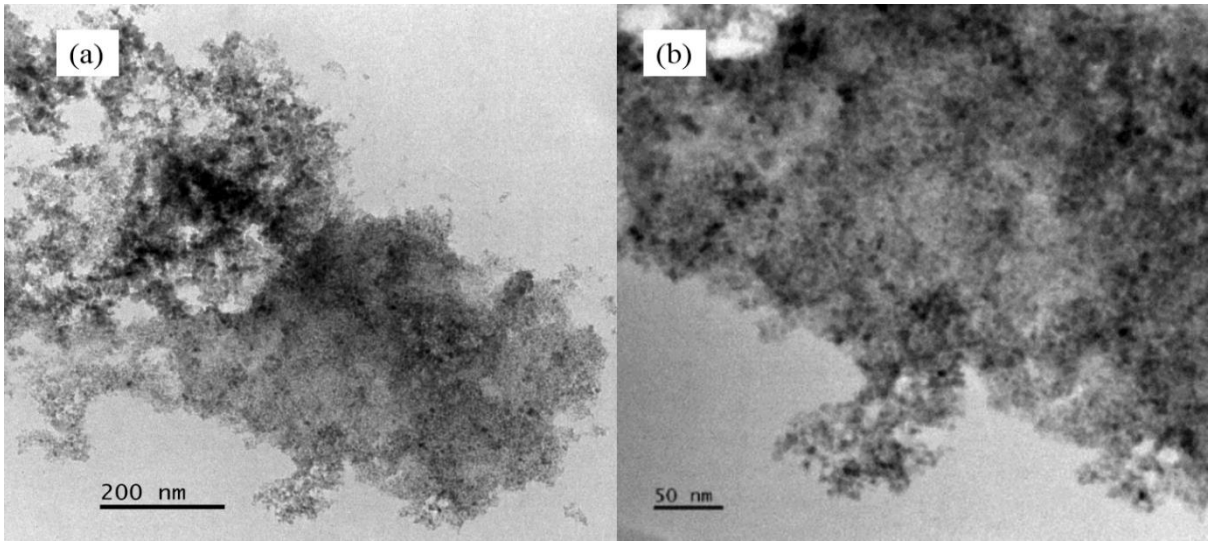

Figure 4.8: TEM images of cobalt sulfide prepared from complex (**5**) at 270 °C at 4 hrs reaction time.

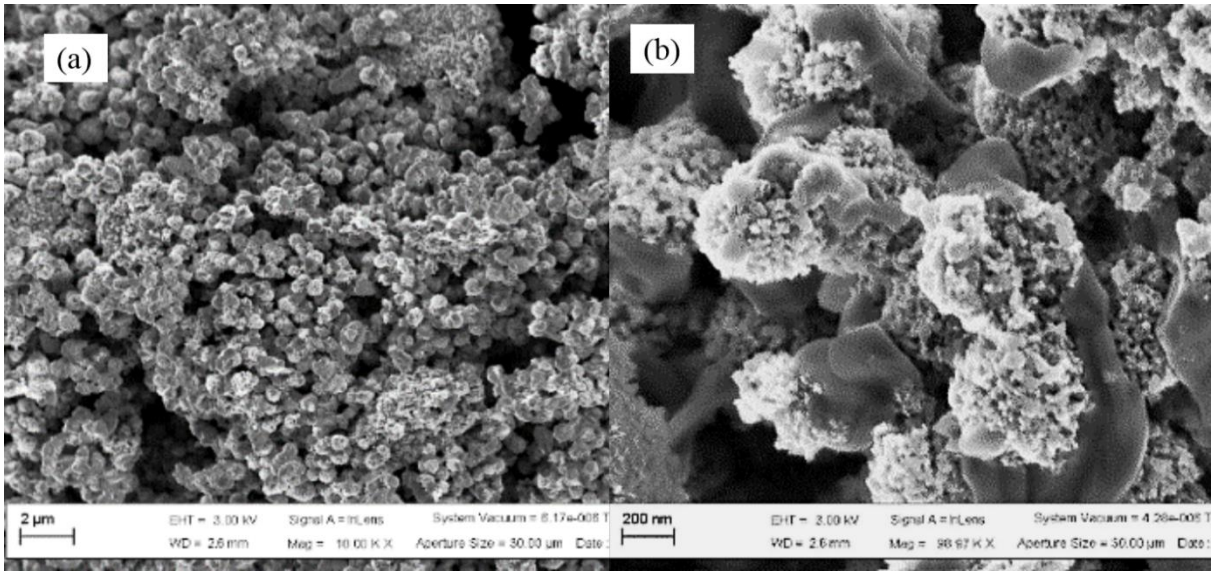

Figure 4.9: (a, b) SEM images of complex (**5**) thermolysed at 270 °C for 4 hrs.

The HR-TEM image (Figure 4.10a) and SAED pattern (Figure 4.10b) of cobalt sulfide nanoparticles obtained from complex (**5**) at 270 °C for 4 hrs. The SAED pattern shows diffraction rings which are indexed to (311), (440) and (400) referenced from the XRD library of Co_3S_4 (ICDD #00-047-1738). HR-TEM image (Figure 4.10a) shows small lattice fringes which make them difficult to measure the lattice spacing.

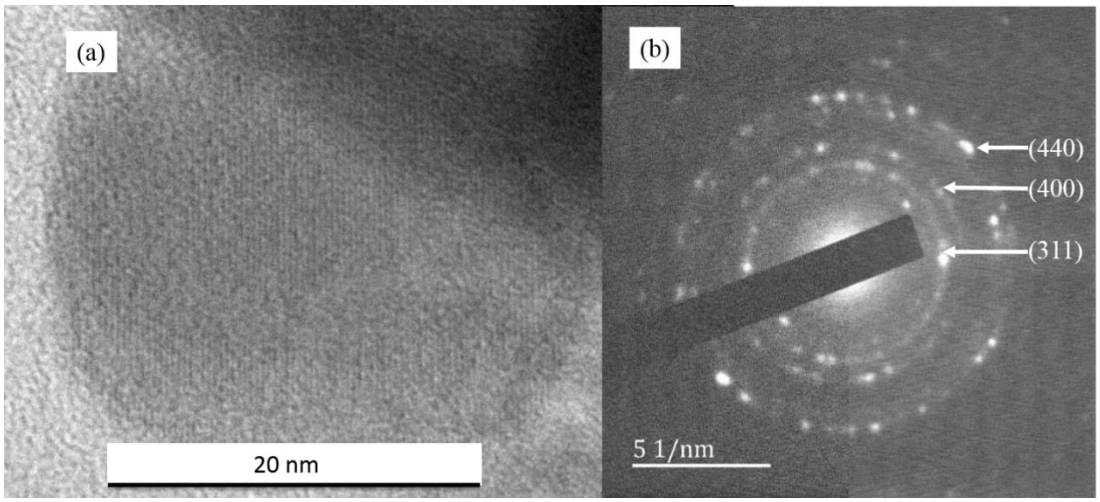

Figure 4.10: (a) HR-TEM image of cobalt sulfide nanoparticles obtained from complex (**5**) at 270 °C for 4 hrs and (b) the corresponding SAED pattern.

Figure 4**.**11 shows the EDX of cobalt sulfide nanoparticles obtained from complex (**5**), the atomic percentage of the chemical composition of cobalt and sulfur are 42.3 % (Co) and 57.7 % (S) with the weight percentages summarized in Table 4.2. The atomic percentage on the EDX image is very close to the ratio of the compound which is 3:4 (Co:S) as expected.

Figure 4.12 is the XRD pattern of cobalt sulfide nanoparticles from the as-prepared sample (complex **5**) obtained for 4 hrs reaction time at 270 °C. All main reflection peaks are indexed to cubic Co_3S_4 which is consistent with those reported values of bulk Co_3S_4 (ICDD #00-047-1738). The average crystallite size is 14.1 nm obtained from the (311) peak.

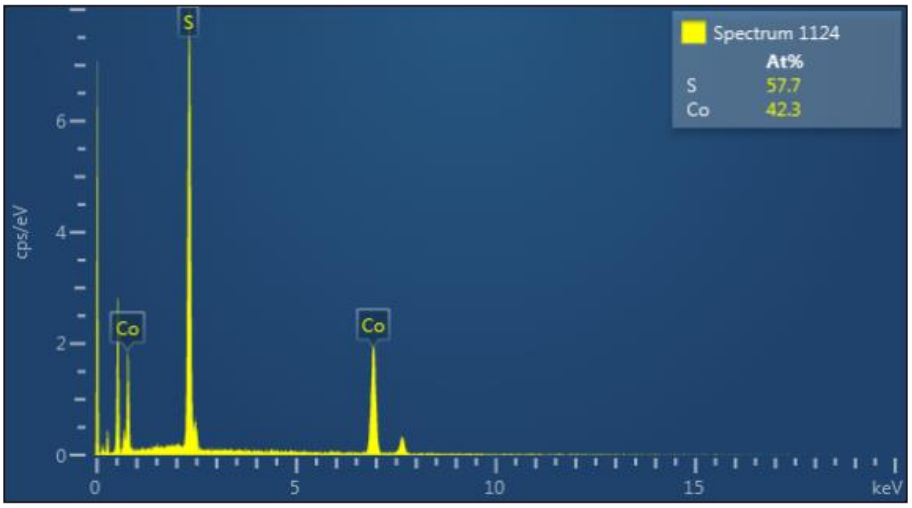

Figure 4.11: EDX patterns of complex (**5**) thermolysed at 270 °C at 4 hrs reaction time.

Table 4.2: Weight and atomic percentage of cobalt and sulfur prepared from complex (**5**).

Time (hrs)	Weight %		Atomic %	
	Cobalt (Co)	Sulfur (S)	Cobalt (Co)	Sulfur (S)
4	57.40	42.60	42.30	57.70

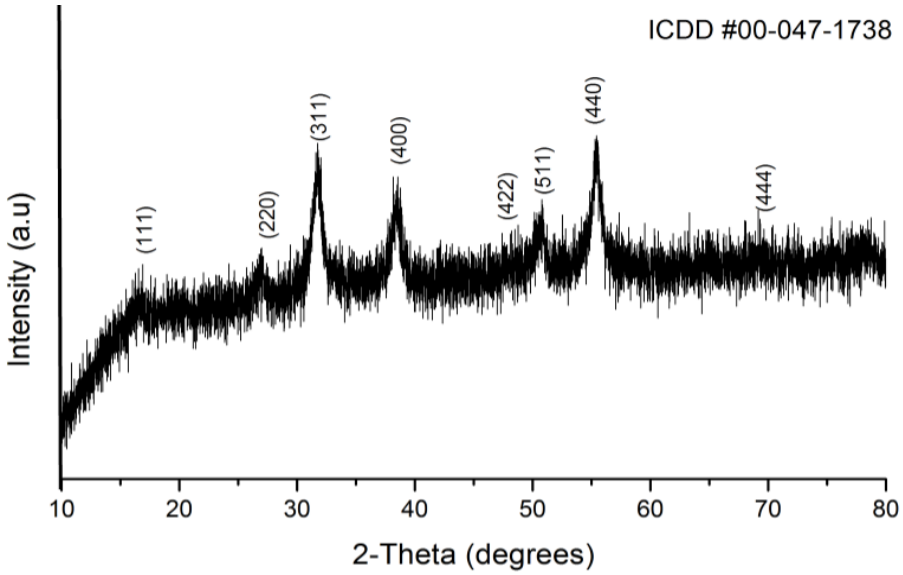

Figure 4.12: X-ray diffraction patterns of cobalt sulfide nanoparticles prepared from complex (**5**) for 4 hrs at 270 °C

4.4. Conclusion

Decomposition of the cobalt Schiff base complexes using1-dodecanethiol as surfactant and as a source of sulfur resulted in the formation of cobalt sulfide nanoparticles. It was found that a change in reaction time and temperature resulted in the formation of different phases such as Co_9S_8 and Co_3S_4. Both SEM and TEM indicated spherical, plate-like and undefined cobalt sulfide nanoparticles whereas EDX showed the presence high percentage of sulfur. The synthesis of cobalt sulfide nanoparticles by using complex (**6**) was never been a success, it gave poor results.

4.5. References

1. C. H. Lai, M. Y. Lu, L. J. Chen; J. Mater. Chem., 22 (2012) 19.
2. A. Wold, K. Dwight; J. Solid State Chem., 96 (1992) 53.
3. T. A. Pecararo, R. R. Chianelli; J. Catal., 67 (1981) 430.
4. Q. R. Hu, S. L. Wang, Y. Zhang, W. H. Tang; J. Alloys Compd. 498 (2010) 707.
5. X. Y. Chen, Z. J. Zhang, Z. G. Qiu, C. W. Shi, X. L. Li; J. Colloid Interface Sci., 308 (2007) 271.
6. A Wold, K Dwight; Solid State Chemistry, New York:Chapman and Hall Inc., (1993).
7. C. N. R. Rao, K. P. R. Pisharody;Prog. Solid State Chem., 10 (1976) 207.
8. S. Bao, Y. Li, C. M. Li, Q. Bao, Q. Lu, J. Guo; Cryst. Growth Des., 8 (10) (2008) 3745.
9. G. B. Smith, A. Ignatiev, G. Zajac; J. Appl. Phys., 51 (1980) 4186.
10. T. M. Whitney, J. S. Jiang, P. Searson, C. Chien; Science, 261 (1993) 1316.
11. G. Wang, S. Zhuo; Phys. Chem. Chem. Phys., 15 (2013) 13801.
12. S. Y. Tai, C. F. Chang, W. C. Liu, J. H. Liao, J. Y. Lin; Electrochim. Acta, 107 (2013) 66.
13. M. S. Faber, K. Park, M. Cabán-Acevedo, P. K. Santra, S. Jin; J. Phys. Chem. Lett. 4 (2013) 1843.
14. C. W. Kung, H. W. Chen, C. Y. Lin, K. C. Huang, R. Vittal, K. C. Ho; ACS Nano., 6 (2012) 7016.
15. H. W. Chen, C. W. Kung, C. M. Tseng, T. C. Wei, N. Sakai, S. Morita, M. Ikegami, T. Miyasaka, K. C. Ho; J. Mater. Chem. A, 1 (2013) 13759.
16. G. H. Yue, P. X. Yan, X. Y. Fan, M. X. Wang, D. M. Qu, Z. G. Wu, C. Li and D. Yan; Electrochem. Solid State Lett., 10 (2007) 29.
17. Q. Wang, L. Jiao, Y. Han, H. Du, W. Peng, Q. Huan, D. Song, Y. Si, Y. Wang, H. Yuan; J. Phys. Chem. C, 115 (2011) 8300.
18. Y. X. Zhou, H. B. Yao, Y. Wang, H. L. Liu, M. R. Gao, P. K. Shen, S. H. Yu; Chem. Eur. J., 16 (2010) 12000.
19. C. Q. Nguyen, A. Adeogun, M. Afzaal, M. A. Malik, P. O'Brien; Chem. Commun., (2006) 2182.
20. N. Revaprasadu, M. A. Malik, P. O'Brien, G. Wakefield; Mater. Res., 14 (08) (1999) 3237.
21. M. A. Malik; J. Mater. Chem., 9 (10) (1999) 2433.
22. M. A. Malik, P. O'Brien; J. Mater. Chem., 9 (11) (1999) 2885.
23. M. Akhtar, J. Akhtar, M. A. Malik, P. O'Brien, F. Tuna, J. Raftery, M. Helliwell; J. Mater. Chem., 21 (26) (2011) 9737.
24. D. J. Binks, S. P. Bant, D. P. Bant, M. A. Malik, P. O'Brien; J. Modern Optics, 50 (2) (2003) 299.
25. W. Maneeprakorn, M. A. Malik, P. O'Brien; J. Mater. Chem., 20 (2010) 2329.
26. K. Ramasamy, M. A. Malik, J. Raftery, F. Tuna, P. O'Brien; Chem. Mater., 22 (2010) 4919.
27. D. E. Bornside, C. W. Macosko, L. E. Scriven; J. Imaging Technol., 13 (1987) 122.
28. N. Kumar, N. Raman, A. Sundaresan; Anorg. Allg. Chem. (2013) Online publication
29. A. S. Pawar, S. S. Garje; Bull, Mater. Sci., 38 (7) (2015) 1843.
30. J. Goldberger, R. He, Y. Zhang, S. Lee, H. Yan, H. J. Choi, P. Yang; Nature, 422 (2003) 599.
31. M. Wirtz, C. R. Martin; Adv. Mater., 15 (2003) 455.
32. K. Ramasamy, M. A. Malik, J. Raftery, P. O'Brien; J. Dalton Trans., 29 (2010) 1460.
33. S. J. Bao, C. M. Li, C. X. Guo, Y. Qiao; J. Power Sources, 180 (2008) 676.

34. L. Zhang, H. B. Wu, X. W. Lou; Chem. Commun., 48 (2012) 6912.
35. G. H. Yue, P. X. Yan, X. Y. Fan, M. X. Wang, D. M. Qu, Z. G. Wu, C. Li, D. Yan; Electrochem. Solid State Lett., 10 (2007) D29.
36. Q. Wang, L. Jiao, H. Du, Y. Si, Y. Wang, H. Yuan; J. Mater. Chem., 22 (2012) 21387.
37. M. Lei, X. L. Fu, H. J. Yang, Y. G. Wang, Y. B. Zhang, P. G. Li; J. Nanosci. Nanotechnol., 12 (2012) 2586.
38. L. D. Nyamen, V. S. Rajasekhar Pullabhotla, A. A. Nejo, P. Ndifon, N. Revaprasadu; New J. Chem., 35 (2011) 1133.
39. J. Chang, C. Cheng, Chem. Commun., 47 (2011) 9089.
40. S. Lee, S. Cho, J. Cheon, Adv. Mater., 15 (5) (2003) 441.
41. P. Scherrer; Math. Phys. Kl., 26 (1918) 98.
42. Y. Waseda, E. Matsubara, K. Shinoda; Springer-Verlag Berlin Heidelberg, (2011) 125.

Chapter 5

Conclusion and Future Prospects

Chapter 5

Conclusion and future prospects

Contents

5.1. Conclusion

New Schiff base ligands have been prepared and subsequently complexed to cobalt(II). Both ligands and complexes which were obtained in good yield (between 70% and 90%) have been characterised using C.H.N/O analyser, FT-IR, H^1 NMR, TGA and DSC. The complexes were investigated as potential single source precursor for synthesis of cobalt and cobalt sulfide nanoparticles (NPs)

The nature of the capping agent and reaction time were parameters which were closely monitored through the quality of Co NPs produced; decomposition temperature of 270 °C was constant throughout. Prior to the thermolysis reactions, the complexes were pyrolyzed at the high temperature (450 °C) thus producing particulates whose morphological and magnetic properties were studied and regarded as reference point to those of the NPs produced. The symmetric complex produced cubic shape nanostructured particulates. The particulates from symmetric complexes exhibited ferromagnetic behaviour, however, the complex (**1**) analogue showed relatively higher coercive fields compared to the complex (**2**) analogue.

In the thermolytic reactions, oleylamine and hexadecylamine were used as capping agents. The former showed not to be a suitable capping agent, since no evidence of NPs formation was observed from the TEM imaging. Rods HDA-capped NPs were obtained from

both symmetric complexes at 2 hrs reaction time. However, the average particle size from the complex (**1**) analogue was, compared 6.55 ± 1.44 nm (width) and 41.38 ± 8.97 nm (length) from the complex (**2**) analogue. An increase in reaction time to 4 hrs gave rectangular to rod shaped NPs; average particle size of 3.31±0.31 nm and 74.06 ±4.2 nm for the diameter and length, respectively from the complex (**1**) analogue and cubic-like NPs from the complex (**2**) analogue were obtained. Therefore, the findings suggest that the nature of the ligand does play a significant role in determining the morphological features of the NPs. However, reaction time has more significant influences in shape transformation of the as-synthesized nanoparticles.

Due to the magnetic properties of Co, the pXRD studies were challenging for the decomposition products obtained from both pyrolysis and thermolysis reactions. Regardless of the decomposition route, only the symmetric analogues gave crystalline products. However, NPs obtained from thermolysis at 2 hrs reaction time showed amorphous behaviour. Pyrolysis produced pure phase Co (PDF Card: 00-015-0608). Thermolysis of the complex (**1**) analogue gave mixed phase NPs indexed to CoO (ICDD #00-043-1004) and Co_3O_4 (ICDD #00-009-0418). The complex (**2**) analogue gave Co NPs of mixed phase, i.e. Co (ICDD #01-088-2325) and Co (ICDD #00-005-0727).

In chapter four the complexes were capped with a sulfur source capping agent to produce cobalt sulfide nanoparticles. The influence of variation in parameters (time) leads to the formation of different phase of cobalt sulfide indexed to cubic Co_9S_8 (ICDD #01-073-6395) and Co_3S_4 (ICDD #00-047-1738) phase. HR-TEM images and SAED patterns of the cobalt sulfide shows planes which are indexed to their relative XRD phases.

5.2. Future prospects

The understanding increased from the preliminary work done in this project could potentially open new opportunities for further research in the use of the new Schiff base complexes (symmetrical and unsymmetrical) as potential precursors towards several synthetic routes to synthesize cobalt and cobalt sulfide nanoparticles, with desired properties for substantial technological and biological applications. The promising pathways to continue the present work are as follows:

- To synthesize tetradentate Schiff base complexes using other metal ions.
- To use these complexes as precursors for other synthetic routes in order to control the growth of the nanoparticles.

- To further study the reaction parameters such as temperature and capping agent (including sulfur source) toward morphological transformation on the particles.

Appendix

1. Research output

Conference

S. H. Khoza and N. Revaprasadu; (2013), Synthesis of Cobalt (II) Schiff bases complexes: Potential precursors for Cobalt nanoparticles, IBSA conference, 27-31 May 2013, Saint George's Hotel and Conference Centre, Centurion, Pretoria, South Africa. (Oral presentation)

Publication

S. H. **Khoza** and N. Revaprasadu; Cobalt Schiff Base Complexes: Single Source Precursor for Cobalt Sulfide (Co_9S_8 and Co_3S_4) Nanoparticles. (Manuscript in preparation)